*DOI:*
10.1021/acsomega.9b03910

*Document Version*
Peer reviewed version

# N1-Benzofused Modification of Fluoroquinolones Reduces Activity Against Gram-Negative Bacteria

Mark Laws[†a], Charlotte Hind[‡a], Andrea Favaron[†⊥], Shirin Jamshidi[†], Bonnie Evans[‡Ψ], Melanie Clifford[‡], J. Mark Sutton*[‡] and Khondaker Miraz Rahman*[†]

[†]Institute of Pharmaceutical Sciences, School of Cancer and Pharmaceutical Sciences, King's College London, Franklin-Wilkins Building, 150 Stamford Street, London, SE1 9NH, UK.

[‡]Public Health England, National Infection Service, Research and Development Institute, Porton Down, Salisbury, Wiltshire, SP4 0JG, UK.

[a]These authors contributed equally to the work.

*Corresponding authors: k.miraz.rahman@kcl.ac.uk; mark.sutton@phe.gov.uk

[⊥]Current address: Department of Pharmaceutical Sciences, University of Padua, Via Francesco Marzolo 5, 35131 Padua, Italy.

[Ψ]Current address: Cancer Research UK Manchester Institute, The University of Manchester, Alderley Park, SK10 4TG, UK.

**Keywords**: Antibiotics, fluoroquinolone, ciprofloxacin, Gram-negative, benzofused, hydrophobicity.

**ABSTRACT**

The fluoroquinolone class of antibiotics have a well-established structure-activity relationship (SAR) and a long history in the clinic, but the effect of electron-rich benzofused substituents at the N1 position remains poorly explored. Since groups at this position are part of the topoisomerase-DNA binding complex and form a hydrophobic interaction with the major groove of DNA, it was hypothesised that an electron-rich benzofused N1 substituent could enhance this interaction. Molecular modelling techniques were employed to evaluate the binding of certain N1-modified fluoroquinolones to DNA gyrase targets from both *Staphylococcus aureus* and *Klebsiella pneumoniae* species compared with ciprofloxacin and norfloxacin. Seven N1-modified fluoroquinolones were subsequently synthesised and tested against a panel of Gram-negative pathogens to determine minimum inhibitory concentration (MIC) values. Gram-negative outer membrane penetration was investigated using the membrane permeabiliser polymyxin B nonapeptide (PMBN) and compound efflux *via* RND-family efflux transporters was evaluated using the known efflux pump inhibitor phenylalanine-arginine beta-naphthylamide (PAβN). Additionally, the target inhibitory activity of representative compound **6e** was determined in a cell-free environment. A correlation between N1 substituent hydrophobicity and activity was observed across the MIC panel, with compound activity decreasing with increased hydrophobicity. Those compounds with highest hydrophobicity were inactive due to poor solubility profiles whereas compounds with intermediate hydrophobicity were inactive due to impaired outer membrane penetration and reduced inhibition of topoisomerase targets, the latter in contrast to modelling predictions. This study adds new information to the fluoroquinolone SAR and suggests limited utility of large hydrophobic substituents at the N1 position of fluoroquinolones.

## INTRODUCTION

Drug design is made far more challenging when structural information about the biological target in question is lacking or the mechanism of action of a hit compound is unknown. While recent advances in the field of protein crystallography have allowed the structures of many challenging targets to be solved[1], molecular modelling has traditionally been employed in such cases to allow the rational design and improvement of promising drug scaffolds[2]. Such modelling originally took the form of ligand-based quantitative structure-activity relationship (QSAR) calculations, used to more effectively rank analogue compounds and optimise scaffolds without offering any specific target information, and now includes target-based molecular docking for which there are various commercially available software suites. Through this, molecular modelling has become a companion technique to traditional compound screening efforts, allowing cheaper and quicker evaluation of chemical libraries against specified targets[2]. The caveat, of course, is that such data is only as useful as the model is accurate. While full quantum mechanical simulations would likely provide the highest degree of accuracy, the extreme computational burden involved in realising such a model on the protein scale continues to make this approach untenable. Instead, modelling suites employ coarse grain molecular dynamics simulations for the majority of the biological target, the more resource-intensive quantum mechanical simulations reserved for small, specific areas with which the drug is likely to directly interact[3]. This compromise inevitably limits the utility of the data generated, the result being that drug discovery efforts are still primarily driven by *in vitro* and *in vivo* assays. Despite this, we opine that the refinement of older, successful drug scaffolds developed in the pre-modelling era represents a task to which current modelling suites are well suited.

One such scaffold is that of the fluoroquinolones. The fluoroquinolones are a family of synthetic, broad-spectrum antibiotic compounds and are important antimicrobial tools within the modern medical arsenal. They remain one of the most frequently prescribed families of antibiotics globally[4] with a combined 17% share of the $43.9bn global antibiotics market in 2014, second only to the β-lactams[5]. Since the discovery of nalidixic acid by Lesher and co-workers in 1962[6], several generations of fluoroquinolone antibiotics have reached the market including ciprofloxacin, levofloxacin and moxifloxacin (Figure 1)[7-8]. However, the class is not without its controversy. The FDA added black box warnings to fluoroquinolone-class drugs in 2008 in response to evidence of increased risk of tendon damage[9] and a number of FDA approved fluoroquinolones including temafloxacin, grepafloxacin and trovafloxacin have either been withdrawn from the clinic or suffered heavily restricted use due to severe adverse effects[10]. Despite further warnings by the FDA in 2013 and then 2016[11], the increasing threat posed by antimicrobial resistance worldwide has stimulated renewed interest in the fluoroquinolones. In June 2017, the FDA approved Melinta Therapeutics' delafloxacin[12]; other quinolones currently in clinical trials include lascufloxacin (Kyorin Pharmaceutical Co. Ltd.), finafloxacin (MerLion Pharmaceuticals Pte Ltd.), nemonoxacin (TaiGen Biotechnology Co. Ltd.), OPS-2071 (Otsuka Pharmaceutical Co. Ltd.) and levonadifloxacin (Wockhardt Ltd.)[13].

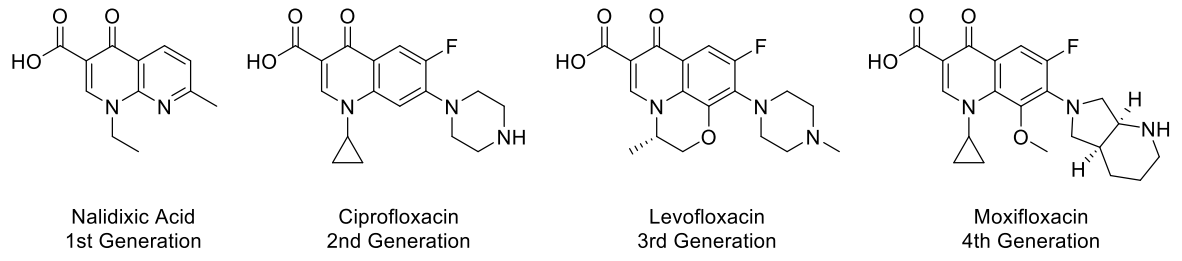


**Figure 1**. Different generations of quinolone family antibiotics. The second generation of quinolones were the first to feature fluorine atoms at the C6 position, hence the adoption of the *fluoro-* prefix for subsequent compounds.

Fluoroquinolones inhibit the actions of DNA gyrase and topoisomerase IV, enzymes that facilitate local introduction or relaxation of DNA supercoils in order to avoid the occurrence of double stranded DNA breaks in the bacterial genome. If the frequency of breaks is high enough to overwhelm cellular DNA repair pathways, cell death occurs[14-18]. To this end, the structure-activity relationship of the quinolone core has been studied in detail to determine substituents that allow for a broad-spectrum activity profile. Groups at the N1 position are part of the topoisomerase-DNA binding complex and form a hydrophobic interaction with the major groove of DNA[19]. A variety of different substituents have found success here, including the cyclopropyl ring present in ciprofloxacin and moxifloxacin (traditionally regarded as the optimal substituent here for potency[20]) and the 3,5-difluoropyridin-2-amine group in the newer delafloxacin, but the effect of large hydrophobic N1 substituents has yet to be fully explored.

We sought to use a molecular modelling-driven approach to investigate the merit of benzofused substituents at the N1 position of the fluoroquinolone nucleus. It was hypothesised that such substituents could present a novel means of enhancing the fluoroquinolone-DNA interaction to improve upon the levels of activity observed in existing fluoroquinolones. To investigate this hypothesis, representative N1-benzofused fluoroquinolones were first docked *in silico* against the DNA gyrase enzymes from *Staphylococcus aureus* and *Klebsiella pneumoniae*, then synthesised using solution phase chemistry and evaluated *in vitro* against panels of clinically relevant Gram-negative pathogens.

## RESULTS AND DISCUSSION

***In Silico* Modelling**. Four novel N1-benzofused fluoroquinolones (**6d-g**) were modelled against the *S. aureus* and *K. pneumoniae* DNA gyrase enzymes. Ciprofloxacin (**6a**), norfloxacin (**6b**) and an N1-benzyl analogue (**6c**) were included as control compounds. The ten most favourable binding poses for each of the seven compounds were selected and compared according to both ChemScore and energy of binding. N1-benzofused compounds were all predicted to possess enhanced binding energy for both gyrase enzymes (best poses ≥ -25.37 kcal/mol versus subunit I) compared to norfloxacin (best poses ≤ -21.54 kcal/mol) and ciprofloxacin (best poses ≤ -23.59 kcal/mol), especially the benzothiophene-containing compounds **6e** (best poses ≥ -27.76 kcal/mol) and **6g** (best poses ≥ -27.20 kcal/mol) (Table S1). Additionally, visual examination of the binding poses predicted for each compound indicated the N1-benzofused compounds would bind *K. pneumoniae* DNA gyrase in a similar manner to ciprofloxacin (Figure 2), though this did not appear to be the case with *S. aureus* (Figure S1). To test these predictions, all seven compounds were synthesised for microbiological evaluation (Scheme 1).

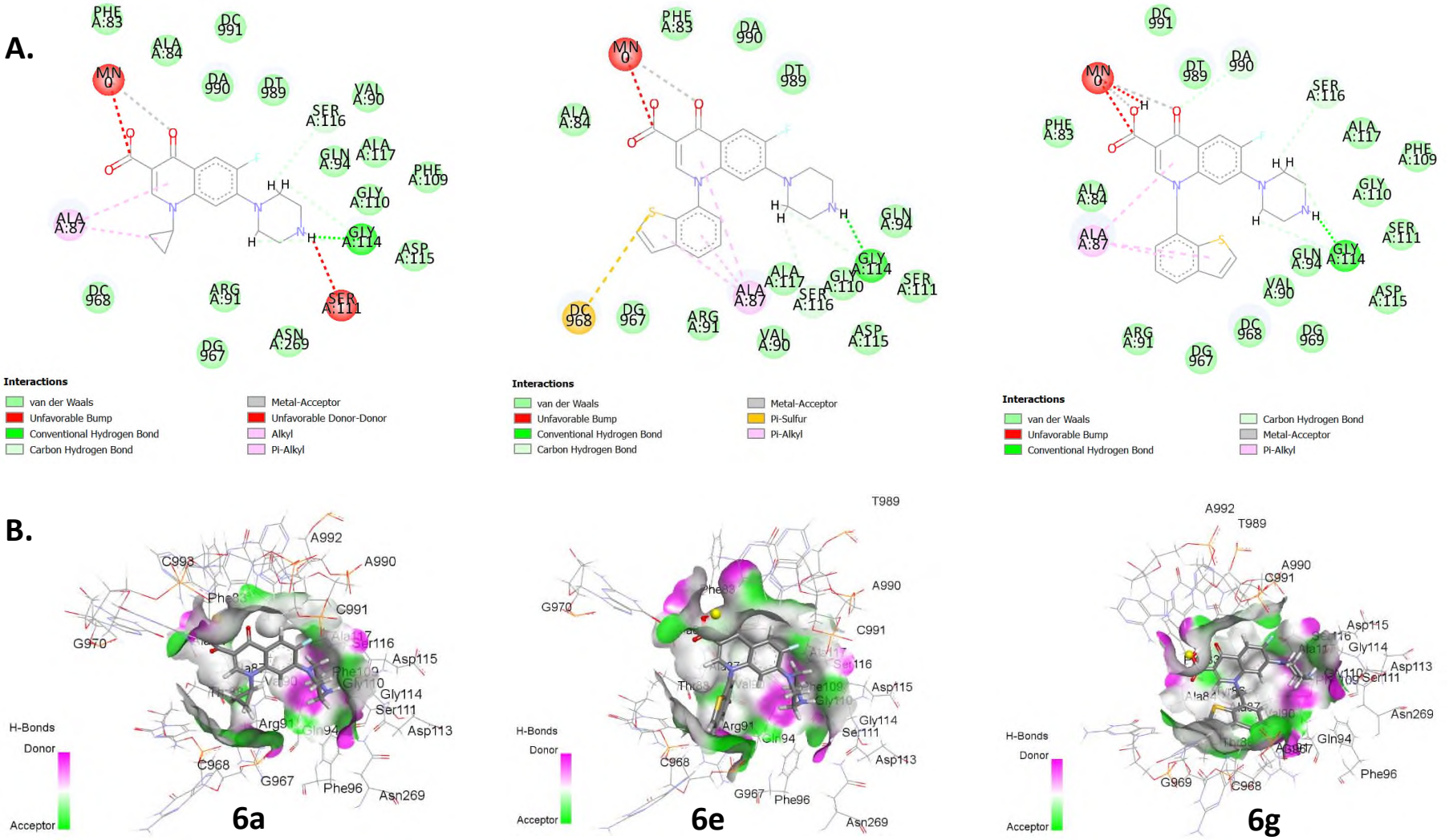


**Figure 2**. (A,B) Molecular modelling results indicate that N1-benzofused compounds (represented by compounds **6e** and **6g**) bind to *K. pneumoniae* DNA gyrase in a similar manner to compound **6a** (ciprofloxacin). Binding poses shown in 2D (A) and 3D (B) views.

## Results

**Chemistry**. Compounds **6a-g** were synthesised using an established solution phase route (Scheme 1) and characterised using LC-MS, HRMS, IR, $^{1}H$ and $^{13}C$ NMR techniques. Hydrochloride salt forms were used to improve aqueous solubility for microbiological testing. clogP values were calculated for each compound (Table 1).

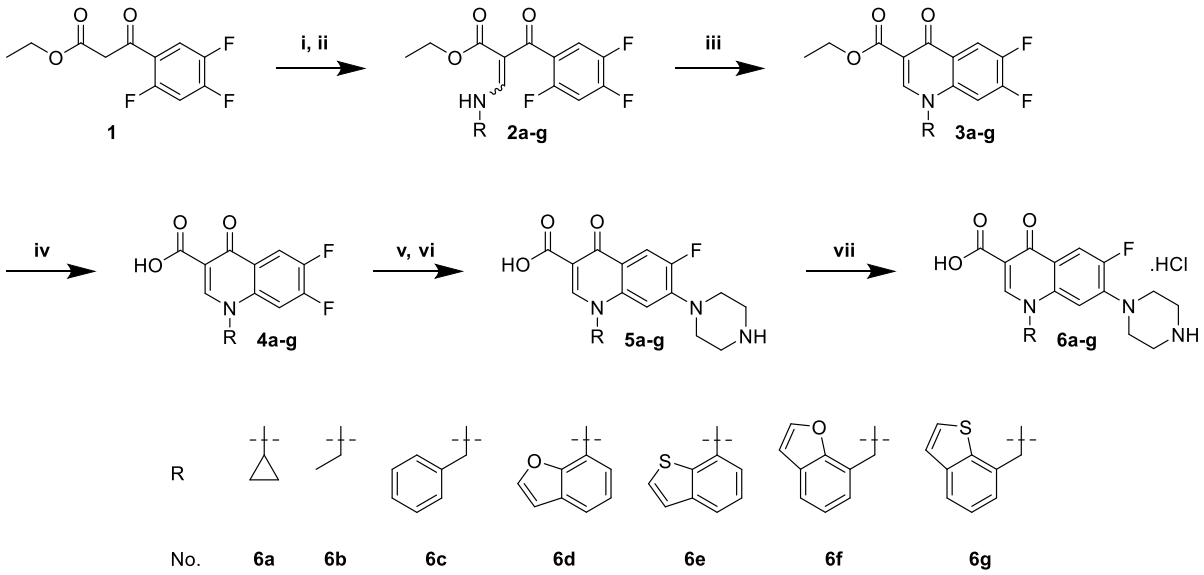


**Scheme 1**. Synthetic scheme used for the preparation of fluoroquinolones including novel N1-benzofused analogues. i) $(EtO)_3CH$, $Ac_2O$, 140°C, 3hrs. ii) R-$NH_2$, DCM, rt, 15hrs. iii) DBU, LiCl, DCM, 45°C – rt, 17.5hrs. iv) HCl, AcOH, reflux, 2.5hrs. v) Boc-piperazine, $K_2CO_3$, DMF, reflux, 15hrs. vi) TFA, dry DCM, rt, 2hrs. vii) 4M HCl in dioxane, DCM, rt, 1hr. The seven fluoroquinolone compounds synthesised as part of this study were three control compounds (ciprofloxacin, norfloxacin and an N-benzyl analogue; **6a-c**) and four novel N1-benzofused analogues (**6d-g**).

**Biological Evaluation**. The antibacterial activities of the synthesised fluoroquinolones were evaluated against a panel of Gram-negative pathogens including *Klebsiella pneumoniae* (NCTC 13368, M6), *Acinetobacter baumannii* (AYE, ATCC 17978), *Pseudomonas aeruginosa* (PAO1, NCTC 13437) and *Escherichia coli* (NCTC 12923, LEC001). The ability

of molecules to permeate the Gram-negative outer membrane was investigated by adding membrane permeabiliser polymyxin B nonapeptide (PMBN) at sub-inhibitory concentrations (Table 2). Phenylalanine-arginine beta-naphthylamide (PAβN) was used to investigate compound efflux by RND-family efflux pumps (Table 3).

| | Compound Code | 6a | 6b | 6c | 6d | 6e | 6f | 6g |
|---|---|---|---|---|---|---|---|---|
| | R |  |  | 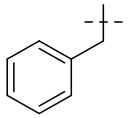 | 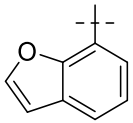 | 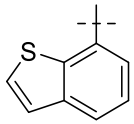 | 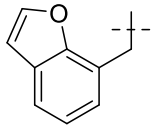 | 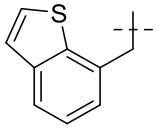 |
| **clogP Calculation Software** | ChemDraw Professional 17.1 | -0.73 | -0.78 | 1.25 | 0.42 | 0.89 | 1.81 | 2.28 |
| | ALOGPS 2.1 | -0.57 | -0.47 | 0.41 | 0.75 | 1.17 | 0.89 | 1.33 |

**Table 1**. clogP values for compounds **6a-g**. Values were calculated using ChemDraw Professional 17.1 and ALOGPS 2.1 software[21], respectively. Refer to Scheme 1 for full structural details.

| | Compound Code | | 6a; ciprofloxacin | | 6b; norfloxacin | | 6c | | 6d | | 6e | | 6f | | 6g | |
|---|---|---|---|---|---|---|---|---|---|---|---|---|---|---|---|---|
| **Species** | **Strain** | **S/R** | -PMBN | +PMBN | -PMBN | +PMBN | -PMBN | +PMBN | -PMBN | +PMBN | -PMBN | +PMBN | -PMBN | +PMBN | -PMBN | +PMBN |
| *K. pneumoniae* | M6 | S | 0.125 | 0.125 | 0.25-0.5 | 0.5 | 1 | 1 | 1-2 | 0.5 | 8 | 2 | >128 | >128 | >128 | >128 |
| | NCTC 13368 | R | 1 | 0.5 | 4 | 2 | 16 | 4 | 16 | 2 | 32 | 8 | >128 | >128 | >128 | >128 |
| *A. baumannii* | ATCC 17978 | S | 0.5 | 0.5 | 8 | 4 | 4-8 | 4 | 2 | 1 | 8 | 4 | >128 | >128 | >128 | >128 |
| | AYE | R | >32 | >32 | >32 | >32 | >32 | >32 | >32 | >32 | >32 | >32 | >128 | >128 | >128 | >128 |
| *P. aeruginosa* | PAO1 | S | 0.5-2 | 0.125 | 2-4 | 0.5 | 8 | 0.5 | 8-16 | 0.5 | 32 | 2 | >128 | 16 | >128 | 32 |
| | NCTC 13437 | R | >32 | 16 | >32 | 32 | >32 | 32 | >32 | 32 | >32 | 32 | >128 | 32 | >128 | 16 |
| *E. coli* | NCTC 12923 | S | ≤0.03 | 0.03-0.06 | 0.125 | 0.125 | 1-2 | 0.5 | 1 | 0.25 | 4 | 1 | >128 | 32 | >128 | 128 |
| | LEC001 | R | 16 | 32 | >32 | >32 | >32 | >32 | >32 | >32 | >32 | >32 | >32 | >32 | >32 | >32 |

**Table 2**. MIC values (mg/L) of synthesised fluoroquinolones. *S/R* refers to strains susceptibility to ciprofloxacin as defined by the EUCAST clinical breakpoints: *S* indicates a strain is ciprofloxacin-sensitive, while *R* indicates a strain is ciprofloxacin-resistant.

| | Compound Code | | 6e | | 6a; ciprofloxacin | |
|---|---|---|---|---|---|---|
| **Species** | **Strain** | **S/R** | -PAβN | +PAβN | -PAβN | +PAβN |
| *K. pneumoniae* | M6 | S | 8 | 1 | ≤0.125 | ≤0.125 |
| | NCTC 13368 | R | >32 | 4 | 0.25 | 0.25 |
| *A. baumannii* | ATCC 17978 | S | 4 | 4 | ≤0.125 | ≤0.125 - 0.5 |
| | AYE | R | >32 | >32 | 32 | >32 |
| *P. aeruginosa* | PAO1 | S | 32 | 2 | ≤0.125 | ≤0.125 |
| | NCTC 13437 | R | >32 | >32 | 32 | 16 |
| *E. coli* | NCTC 12923 | S | 0.25-2 | 0.25 | ≤0.125 | ≤0.125 |
| | LEC001 | R | >32 | >32 | 16 | 32 |

**Table 3**. MIC values (mg/L) of synthesised fluoroquinolone (**6e)** vs. ciprofloxacin (**6a**) in the presence or absence of the efflux pump inhibitor PAβN. *S/R* refers to strains susceptibility to ciprofloxacin as defined by the EUCAST clinical breakpoints: *S* indicates a strain is ciprofloxacin-sensitive, while *R* indicates a strain is ciprofloxacin-resistant.

Across the panel, activity is broadly reduced or abolished in the N1-benzofused analogues compared to ciprofloxacin (**6a**) and norfloxacin (**6b**); MICs against ciprofloxacin-sensitive strains are all ≥4x higher than for ciprofloxacin. The uniformly poor activities of the most hydrophobic compounds **6f** and **6g** are likely a result of their poor solubility profiles.

***Klebsiella pneumoniae***. For the ciprofloxacin-resistant strain NCTC 13368, PMBN rescues the activities of compounds **6d** and **6e** by 4-8-fold compared to the 2-fold difference seen for both norfloxacin and ciprofloxacin. This pattern extends to the ciprofloxacin-sensitive strain M6 (2-4-fold versus 1-fold potentiation). Using compound **6e** as a reference compound, these strains also show significant potentiation with the RND-family efflux inhibitor PAβN, suggesting that the compounds are susceptible to efflux. This was not evident for ciprofloxacin.

***Acinetobacter baumannii***. The trend observed in both *K. pneumoniae* strains extends to the ciprofloxacin-sensitive *A. baumannii* strain ATCC 17978, with **6d** and **6e** potentiated 2-fold by PMBN versus 1-2-fold for ciprofloxacin and norfloxacin. The ciprofloxacin-resistant strain AYE remains highly resistant to all compounds tested, likely due to mutations in *gyrA*. Neither ciprofloxacin nor compound **6e** showed any difference in MIC when treated in the presence of PAβN.

***Pseudomonas aeruginosa***. The aforementioned trend is also visible in ciprofloxacin sensitive *P. aeruginosa* strain PAO1, with PMBN potentiating **6d** and **6e** 16->32-fold versus 4-16-fold for norfloxacin and ciprofloxacin. Unlike for both *K. pneumoniae* and *A. baumannii*, the activities of **6f** and **6g** were also rescued by over 8-fold against both strains, though all MICs remain well above the EUCAST clinical breakpoint for ciprofloxacin. PAO1, but not NCTC 13437, showed significant potentiation with PAβN.

***Escherichia coli***. PMBN rescues the activity of all analogues by 2->8 fold versus 1->4-fold for norfloxacin and ciprofloxacin. No effect was observed with PAβN for either compound **6e** or ciprofloxacin.

*In vitro* activity assays using purified *S. aureus*, *E. coli* and *P. aeruginosa* DNA gyrase and *S. aureus* topoisomerase IV enzymes were performed in order to evaluate whether the gains in inhibitory activity predicted for the benzofused compounds were accurate. The benzothiophene-containing **6e** was selected as a representative compound for the purposes of this experiment. Results indicate that **6e** has a markedly reduced inhibitory activity for the *E. coli* and *P. aeruginosa* enzymes (**6e** $IC_{50}$ = 2.70 µg/mL ± 0.42 and 6.68 µg/mL ± 1.46, respectively) compared to ciprofloxacin ($IC_{50}$ = 0.069 µg/mL ± 0.01 and 0.11 µg/mL ± 0.01, respectively) (Figure 3). An accurate $IC_{50}$ could not be determined for compound **6e** against the *S. aureus* DNA gyrase or topoisomerase IV enzymes because the compound was poorly soluble in the assay media at the high concentrations required.

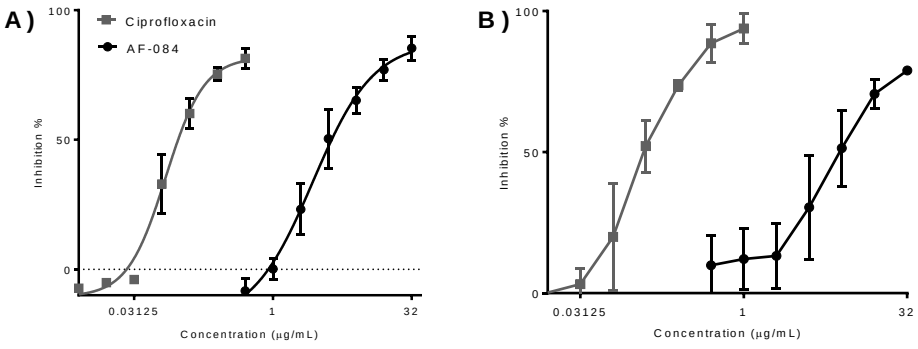


**Figure 3**. $IC_{50}$ analysis for **6e** against A) *E. coli* DNA gyrase and B) *P. aeruginosa* DNA gyrase.

**Discussion**. A general correlation between N1 substituent hydrophobicity and activity is observed; compounds **6c**, **6d** and **6e** are of intermediate hydrophobicity and display limited activity, whereas the more hydrophobic **6f** and **6g** show almost complete loss of activity versus ciprofloxacin. Compounds **6d** and **6e** are less active in *K. pneumoniae*, *P. aeruginosa* and *E. coli* due to impaired outer membrane penetration, as evidenced by greater potentiation by PMBN versus ciprofloxacin and norfloxacin, lower inhibitory activity for DNA gyrase, as indicated by the *E. coli* and *P. aeruginosa* $IC_{50}$s of **6e**, and – in the case of *P. aeruginosa* PAO1 and both *K. pneumoniae* strains – efflux by RND-family efflux pumps, as evidenced by conducting MICs for **6e** with and without the efflux pump inhibitor PAβN. The outer membrane of *A. baumannii* strain ATCC 17978 does not seem to impede compound influx in the same way as described above and we can conclude that higher MIC values in the benzofused compounds in this strain are solely due to lower inhibitory activity. The uniformly poor activities of the most hydrophobic compounds **6f** and **6g** indicate that these analogues are chiefly affected by poor solubility profiles, as was evidenced when undertaking the MIC experiments. None of the N1-benzofused analogues showed superior activity to ciprofloxacin in ciprofloxacin-resistant strains, indicating that the resistance mechanisms that afflict ciprofloxacin in these bacteria are no less effective against the benzofused analogues.

Comparison of the molecular modelling and *in vitro* data highlights several important points. The weakness of any molecular model lies in the variables excluded from it; since whole-cell systems are far too large and complex to model currently, the lack of a membrane component to simulate compound influx remains a key shortcoming in antibacterial docking efforts. However, this does not mean that the predicted gains in gyrase inhibition are incorrect. For compounds **6d** and **6e** which were capable of influx into certain strains of bacteria, the problem may be that the ChemScore and binding energy parameters used in the docking are poorly

suited to determining whether a fluoroquinolone will inhibit the topoisomerase target. While both parameters offer a guide to the most preferable binding pose of a drug by assessing a plethora of non-covalent binding interactions, neither considers the individual importance of said interactions beyond their relative contributions to likely binding energy. Specifically, fluoroquinolones inhibit topoisomerase enzymes by forming a C3 carboxylate magnesium-water bridge with aspartic/glutamic acid and serine residues in the GyrA/ParC enzyme subunits. Therefore, it is plausible that N1-benzofused analogues **6d** and **6e** do possess higher binding energies for the enzyme but show reduced inhibition of it due to an altered binding pose. We recommend that this possibility be considered in all future modelling efforts with novel fluoroquinolones. This study illustrates that while molecular modelling is a useful technique in drug design, it cannot yet be a full substitute for traditional *in vitro* and *in vivo* compound screening efforts.

## MATERIALS AND METHODS

### Synthetic Organic Chemistry

***General***. Synthetic building blocks and reagents were purchased from a number of suppliers including Fluorochem (UK), Sigma-Aldrich (Merck KGaA, USA), Thermo Fisher Scientific (UK, including Acros Organics, Maybridge and Alfa Aesar), Activate Scientific (UK), Enamine (Ukraine), VWR International (USA), Oxchem (USA) and Apollo Scientific (UK). Solvents were purchased from Sigma-Aldrich and Thermo Fisher Scientific. Thin-layer chromatography (TLC) analysis was performed using silica gel plates (Merck silica gel 60 F254 plates) and visualised using ultraviolet (UV) light (254 nm wavelength) and/or staining with potassium permanganate solution. Manual flash column chromatography was performed using silica gel (Merck 9385, 230-400 mesh ASTM, 40-63 µM) as the stationary phase. TLC was employed to discern solvent systems (mobile phases) with appropriate separation profiles;

said profiles were comprised of hexanes and ethyl acetate. Liquid chromatography–mass spectrometry (LC-MS) was employed to monitor reaction progression and compound identification. LC-MS analysis was performed on a Waters Alliance 2695 HPLC coupled to a Waters Micromass ZQ instrument with a Waters 2996 PDA. For liquid chromatography, an Onyx™ Monolithic C18 column (50 x 4.6 mm) was used and the mobile phases were comprised of water (A) and acetonitrile (B). Formic acid (0.1%) was added to both to ensure acidic conditions throughout the analysis. Gradient conditions used were as follows. Method A (5 min): from 95% A/5% B to 90% B over 3 min. Then from 90% B to 95% B over 0.5 min and held constant for 1 min. This was then reduced to 5% B over 0.5 min. The flow rate was 1.0 mL/min, 100 μL was split *via* a zero dead volume T piece which passed into the mass spectrometer. The wavelength range of the UV detector was 220-500 nm. Method B (10 min): from 95% A/5% B to 50% B over 3 min. Then from 50% B to 80% B over 2 min. Then from 80% B to 95% B over 1.5 min and held constant for 1.5 min. This was then reduced to 5% B over 0.2 min and maintained to 5% B for 1.8 min. The flow rate was 0.5 mL/min, 200 μL was split *via* a zero dead volume T piece which passed into the mass spectrometer. The wavelength range of the UV detector was 220-400 nm. Mass spectrometry data (both ESI+ and ESI- modes) were collected using the following Waters Micromass ZQ parameters: capillary (kV), 3.38; cone (V), 35; extractor (V), 3.0; source temperature (°C), 100; de-solvation temperature (°C), 200; cone flow rate (L/h), 50; de-solvation flow rate (L/h), 250. High resolution mass spectra were obtained on a Thermo Navigator mass spectrometer coupled with liquid chromatography (LC) using electrospray ionisation (ES) and time-of-flight (TOF) mass spectrometry. Infrared spectra (IR) were recorded on a Perkin Elmer spectrum 1000 instrument. All NMR spectra were obtained at room temperature using a Bruker Ascend 400 MHz NMR spectrometer and interpreted using ACD/NMR Processor Academic Edition software. Chemical shifts (δ H) are expressed in parts per million (ppm) relative to deuterated chloroform ($CDCl_3$, residual signal

$^{1}$H δ = 7.26, $^{13}$C δ = 77.2), deuterated dimethyl sulfoxide ($(CD_3)_2SO$, residual signal $^{1}$H δ = 2.54, $^{13}$C δ = 40.5) or deuterated trifluoroacetic acid ($CF_3CO_2D$, residual signal $^{1}$H δ = 11.50, $^{13}$C δ = 164.4, 116.5). Coupling constants are expressed in Hz. Multiplicities in $^{1}$H NMR spectra are quoted as s = singlet, d = doublet, t = triplet, q = quartet, m = multiplet, dd = doublet of doublets, ddd = doublet of doublet of doublets, dt = doublet of triplets, td = triplet of doublets, spt = septet and br = broad.

**Microbiological Evaluation**

***Minimal Inhibitory Concentrations (MICs)***. Minimal inhibitory concentrations (MICs) were determined using the microdilution broth method. Briefly, compounds were added to the first two columns of a 96-well plate and diluted two-fold down the plate in tryptic soy broth (TSB). Overnight cultures of bacteria were then adjusted to a concentration of $1x10^6$ CFU/mL and added to each well for a final concentration of $5x10^5$ CFU/mL. The MIC was defined as the lowest concentration of compound which resulted in no visible growth at an optical density of 600 nm after 20 hours incubation at 37°C. Where necessary, MIC determinations were carried out in the presence of the membrane permeabiliser polymyxin B nonapeptide (PMBN) at a final concentration of 30 μg/mL, or an efflux pump inhibitor, PAβN, at a final concentration of 25 μg/mL, concentrations which did not affect bacterial growth.

***Gyrase Inhibition Assay***. DNA gyrase from *S. aureus* and *E. coli* were treated with compound **6e** and the positive control ciprofloxacin using the cell-free *S. aureus*, *E. coli* and *P. aeruginosa* gyrase supercoiling kits (#SAS4001, K0001, PAS001), and the *S. aureus* topoisomerase IV relaxation kit (SAR4001), all obtained from Inspiralis (Norwich, UK), according to manufacturer's instructions, as described previously[22-23].

**Molecular Modelling**

***Generation of Structures***. PDB ID code 2XCT was used for the 3D structure of *Staphylococcus aureus* GyrA. The structure of *Klebsiella pneumoniae* GyrA was generated by homology modelling using the FASTA UniProt code A0A0C7K6P2. The sequence identity between the target and template protein with PDB ID code 4TMA was 96.57% for *K. pneumoniae* GyrA. The final structures of the gyrase and associated DNA structures were amended and assembled using Accelrys Discovery Studio. The 3D structures of ligands were generated using Chem3D 15.0 software and the structures were minimised with SYBYL.

***Molecular Docking***. Molecular docking was performed to generate several distinct binding orientations and the binding affinity for each binding mode. Subsequently the binding modes that showed the highest score and lowest binding energy were considered as the most favourable binding modes. AutoDock SMINA was used for blind molecular docking of the ligands to gyrase enzymes to find the best binding pocket by exploring all probable binding cavities in the enzymes. All parameters were kept at their default values for running SMINA. GOLD was then used for molecular docking of the compounds into the SMINA-located binding site for performing flexible molecular docking and determining more precise energies and scores. Based on fitness function score and ligand binding position, the best-docked pose for each compound was selected; high fitness function scores (generated using GOLD) and low binding energy values are indicative of the best-docked pose for each system. A genetic algorithm (GA) is used in GOLD ligand docking to thoroughly examine the ligand conformational flexibility along with the partial flexibility of the protein. The maximum number of runs was set to 20 for each compound, and the default parameters were selected (100 population size, 5 for the number of islands, 100,000 number of operations and 2 for the niche size). Default cutoff values of 2.5 Å (dH-X) for hydrogen bonds and 4.0 Å for van-der-

Waals distance were employed. When the top solutions attained the RMSD values within 1.5 A˚, the GA docking was terminated.

## CONCLUSION

This study suggests large hydrophobic groups, particularly aromatic benzofused rings, have limited utility at the N1 position of fluoroquinolones as they significantly alter the physicochemical and drug-like properties of the molecules. Electron-rich, hydrophobic, benzofused substitutions negatively impact penetration of the Gram-negative outer membrane in *K. pneumoniae*, *P. aeruginosa* and *E. coli* and do not afford protection from existing fluoroquinolone resistance mechanisms present in these species. These modifications also reduce target inhibition (other factors, including substituent size and geometry, are clearly intrinsic determinants of biological activity) and compound solubility in aqueous media. However, the modifications considered herein may not represent the full potential of such modifications; more highly functionalised, polar heteroaromatic groups may yet prove promising N1 substituents for the next generation of fluoroquinolones. The findings also suggest that, while still a powerful technique, molecular modelling alone was unable to successfully predict improvements to the fluoroquinolone scaffold at the N1 position, both due to considerations outside of the scope of the model (membrane penetration, compound solubility) and inaccuracies inherent to current modelling techniques (poor prediction of compound affinity for target with regards to inhibition).

## EXPERIMENTAL SECTION

**General Procedure for Compounds 2a – g**. Ethyl 2,4,5-trifluorobenzoylacetate (**1**; 1 g, 4.06 mmol, 1 eq.) was dissolved in triethyl orthoformate (1.15 mL, 6.90 mmol, 1.7 eq.) and heated at 140 °C for 30 minutes. Acetic anhydride (1.15 mL, 12.19 mmol, 3 eq.) was added and the mixture refluxed at 140 °C for another 3 hours. Upon completion, the reaction was cooled to room temperature, DCM (3 mL) was added and the mixture was stirred at room temperature for 10 minutes. Then cyclopropylamine (703 μL, 10.15 mmol, 2.5 eq.) was added and the reaction was stirred at room temperature until completion. The crude was concentrated *in vacuo* and the resulting solid was dissolved in DCM (2 mL) and purified by flash chromatography (50% Hex/50% EtOAc) to yield compound **2a**, pale yellow solid, 1.158 g (91.0% yield); $^{1}$H NMR (400 MHz, $CDCl_3$) δ 10.87 (d, *J* = 12.59 Hz, 0.75H, H4), 9.42 (d, *J* = 13.60 Hz, 0.25H, H4), 8.20 (d, *J* = 13.85 Hz, 0.75H, H3), 8.16 (d, *J* = 14.35 Hz, 0.25H, H3), 7.33 (ddd, *J* = 10.07, 8.81, 6.29 Hz, 0.25H, H1), 7.19 (ddd, *J* = 9.82, 8.81, 6.29 Hz, 0.75H, H1), 6.83 - 6.91 (m, 1H, H2), 4.05 (q, *J* = 7.13 Hz, 1.5H, H8), 4.00 (q, *J* = 7.05 Hz, 0.5H, H8), 2.92 - 3.02 (m, 1H, H5), 1.08 (t, *J* = 7.18 Hz, 2.25H, H9), 0.77 - 0.97 (m, 4.75H, H6+7+9); $^{13}$C NMR (101 MHz, $CDCl_3$) δ 188.1, 186.0, 168.4, 166.6, 160.8, 160.4, 154.1 (ddd, 247.22, 9.54, 2.94 Hz), 150.5 (ddd, 253.09, 14.67, 12.47 Hz), 146.6 (ddd, 245.02, 12.47, 3.67 Hz), 127.2 - 127.6 (m), 117.7 (ddd, *J* = 20.54, 5.13, 1.47 Hz), 116.8 (ddd, *J* = 20.54, 5.13, 1.47 Hz), 105.1 (dd, *J* = 28.61, 21.27 Hz), 104.9 (dd, *J* = 28.61, 21.27 Hz), 101.6, 101.6, 59.9, 59.6, 30.4, 30.1, 14.0, 13.6, 6.6, 6.5; ($\upsilon_{max}$/cm$^{-1}$) 1686, 1623, 1569, 1508, 1426, 1406, 1357, 1330, 1294, 1244, 1228, 1174, 1136, 1088, 1058, 1033, 1015, 890, 877, 809, 797, 773, 754, 734, 660, 588. **See note A**.

Compound **2b**, pale yellow solid, 4.916 g (80.3% yield); $^{1}$H NMR (400 MHz, $CDCl_3$) δ 10.89 (br. s., 0.8H, H4), 9.40 (br. s., 0.2H, H4), 8.12 (d, *J* = 14.10 Hz, 0.8H, H3), 8.10 (d, *J* = 14.60 Hz, 0.2H, H3), 7.32 (ddd, *J* = 9.82, 8.81, 6.29 Hz, 0.2H, H1), 7.19 (ddd, *J* = 9.82, 8.81, 6.29 Hz, 0.8H, H1), 6.81 - 6.92 (m, 1H, H2), 4.05 (q, *J* = 7.18 Hz, 1.6H, H7), 4.00 (q, *J* = 7.18

Hz, 0.4H, H7), 3.44 - 3.55 (m, 2H, H5), 1.36 (t, *J* = 7.30 Hz, 2.4H, H6), 1.33 (t, *J* = 7.30 Hz, 0.6H, H6), 1.07 (t, *J* = 7.18 Hz, 2.4H, H8), 0.94 (t, *J* = 7.18 Hz, 0.6H, H8); $^{13}$C NMR (101 MHz, $CDCl_3$) δ 188.0, 168.6 (d, *J* = 1.47 Hz), 166.8 (d, *J* = 1.47 Hz), 160.2, 160.0, 159.8, 154.1 (ddd, *J* = 247.22, 9.54, 2.20 Hz), 150.4 (ddd, *J* = 253.09, 14.67, 12.47 Hz), 146.6 (ddd, *J* = 245.02, 13.20, 3.67 Hz), 127.4 - 127.7 (m), 116.7 (ddd, *J* = 20.54, 5.87, 1.47 Hz), 105.0 (dd, *J* = 28.61, 20.54 Hz), 101.0, 100.8, 59.8, 59.5, 45.1, 44.9, 44.8, 15.8, 15.7, 15.7, 14.0, 13.6; ($\upsilon_{max}$/$cm^{-1}$) 1678, 1622, 1560, 1510, 1428, 1415, 1380, 1364, 1330, 1310, 1283, 1244, 1219, 1175, 1156, 1136, 1092, 1050, 1036, 884, 1015, 863, 829, 800, 774. **See note A**.

Compound **2c**, pale yellow solid, 1.039 g (70.7% yield); $^1$H NMR (400 MHz, $CDCl_3$) δ 11.10 (br. s., 0.75H), 9.63 (br. s., 0.25H), 8.14 - 8.23 (m, 1H), 7.34 - 7.45 (m, 3H), 7.27 - 7.33 (m, 2H), 7.21 (ddd, *J* = 10.01, 8.75, 6.17 Hz, 1H), 6.83 - 6.92 (m, 1H), 4.58 - 4.64 (m, 2H), 4.06 (q, *J* = 7.05 Hz, 1.5H), 4.01 (q, *J* = 7.05 Hz, 0.5H), 1.08 (t, *J* = 7.05 Hz, 2.25H), 0.95 (t, *J* = 7.05 Hz, 0.75H); $^{13}$C NMR (101 MHz, $CDCl_3$) δ 188.3, 166.7, 160.4, 160.0, 135.7, 135.5, 129.1, 129.1, 128.5, 128.4, 127.5, 127.5, 116.8 (ddd, *J* = 1.47, 5.14, 20.54 Hz), 105.1 (dd, *J* = 21.27, 28.61 Hz), 105.0 (dd, *J* = 21.27, 28.61 Hz), 101.6, 101.5, 59.9, 59.6, 54.0, 53.8, 14.0, 13.6; ($\upsilon_{max}$/$cm^{-1}$) 1676, 1628, 1604, 1434, 1379, 1366, 1329, 1311, 1301, 1231, 1175, 1139, 1050, 1019, 855, 844, 802, 777, 732, 721, 692, 652, 580. **See notes A, B**.

Compound **2d**, white solid, 1.260 g (79.7% yield); $^1$H NMR (400 MHz, $CDCl_3$) δ 12.83 (d, *J* = 13.85 Hz, 0.66H), 11.46 (d, *J* = 13.60 Hz, 0.33H), 8.99 (d, *J* = 13.60 Hz, 0.66H), 8.85 (d, *J* = 13.85 Hz, 0.33H), 7.74 (d, *J* = 2.27 Hz, 0.66H), 7.72 (d, *J* = 2.01 Hz, 0.33H), 7.44 - 7.51 (m, 1H), 7.42 (dd, *J* = 7.81, 1.01 Hz, 0.33H), 7.36 (ddd, *J* = 9.82, 8.81, 6.29 Hz, 0.66H), 7.24 - 7.31 (m, 1H), 7.20 - 7.24 (m, 0.66H), 7.16 - 7.20 (m, 0.33H), 6.92 (m, 1H), 6.86 (d, *J* = 2.01 Hz, 0.66H), 6.84 (d, *J* = 2.27 Hz, 0.33H), 4.12 - 4.19 (m, 2H), 1.15 (t, *J* = 7.18 Hz, 2H), 1.04 (t, *J* = 7.18 Hz, 1H); $^{13}$C NMR (101 MHz, $CDCl_3$) δ 189.0, 186.3, 168.2, 166.5, 154.5 (ddd, *J* = 2.93, 9.54, 247.95 Hz), 153.4, 152.5, 151.0 (ddd, *J* = 12.47, 14.67, 254.56 Hz), 146.7 (ddd,

*J* = 3.67, 12.47, 245.75 Hz), 145.8, 145.7, 145.0, 144.8, 129.5, 129.4, 126.8 - 127.0 (m), 124.2, 123.9, 123.8, 118.6, 118.0 - 118.2 (m), 118.0, 117.2 (ddd, *J* = 1.47, 5.13, 20.54 Hz), 112.4, 111.5, 107.2, 105.2 (dd, *J* = 21.27, 28.61 Hz), 105.1 (dd, *J* = 21.27, 28.61 Hz), 104.8, 104.3, 60.3, 60.2, 14.0, 13.7; ($\upsilon_{max}$/$cm^{-1}$) 1701, 1624, 1596, 1567, 1506, 1448, 1428, 1307, 1251, 1207, 1179, 1136, 1085, 1060, 1031, 1015, 976, 877, 812, 786, 729, 618, 599, 586, 566, 535, 519. **See notes A, B**.

Compound **2e**, yellow solid, 1.354 g (86.5% yield); $^{1}$H NMR (400 MHz, $CDCl_3$) δ 12.80 (d, *J* = 13.35 Hz, 0.66H), 11.31 (d, *J* = 13.60 Hz, 0.33H), 8.78 (d, *J* = 13.09 Hz, 0.66H), 8.66 (d, *J* = 13.60 Hz, 0.33H), 7.75 (dd, *J* = 7.93, 0.63 Hz, 0.66H), 7.71 (dd, *J* = 7.93, 0.63 Hz, 0.33H), 7.55 (dd, *J* = 5.29, 0.50 Hz, 0.66H), 7.53 (dd, *J* = 5.29, 0.50 Hz, 0.33H), 7.43 - 7.50 (m, 2H), 7.28 - 7.43 (m, 2H), 6.88 - 6.97 (m, 1H), 4.13 - 4.21 (m, 2H), 1.16 (t, *J* = 7.18 Hz, 2H), 1.05 (t, *J* = 7.18 Hz, 1H); $^{13}$C NMR (101 MHz, $CDCl_3$) δ 189.1, 186.3, 168.3, 166.3, 153.2, 152.4, 141.7, 141.6, 133.9, 133.8, 131.0, 126.7, 126.4, 125.6, 125.5, 124.9, 124.8, 121.7, 121.1, 117.2 (ddd, *J* = 1.47, 5.14, 20.54 Hz), 112.6, 111.8, 105.2 (dd, *J* = 21.27, 28.61 Hz), 105.2 (dd, *J* = 21.27, 28.61 Hz), 104.4, 60.4, 60.3, 14.0, 13.7; ($\upsilon_{max}$/$cm^{-1}$) 1693, 1620, 1595, 1507, 1435, 1383, 1324, 1293, 1248, 1186, 1139, 1100, 1020, 978, 893, 787, 761, 734 701, 666, 593, 564. **See notes A, B**.

Compound **2f**, pale yellow solid, 491 mg (85.7% yield); $^{1}$H NMR (400 MHz, $CDCl_3$) δ 11.10 - 11.32 (m, 0.75H), 9.64 - 9.81 (m, 0.25H), 8.32 (d, *J* = 13.85 Hz, 0.75H), 8.28 (d, *J* = 14.35 Hz, 0.25H), 7.68 - 7.72 (m, 1H), 7.60 - 7.64 (m, 1H), 7.33 (ddd, *J* = 10.07, 8.81, 6.29 Hz, 0.25H), 7.16 - 7.30 (m, 3H), 6.82 - 6.91 (m, 2H), 4.86 - 4.92 (m, 2H), 4.07 (q, *J* = 7.05 Hz, 1.5H), 4.00 (q, *J* = 7.05 Hz, 0.5H), 1.08 (t, *J* = 7.05 Hz, 2.25H), 0.94 (t, *J* = 7.05 Hz, 0.75H); $^{13}$C NMR (101 MHz, $CDCl_3$) δ 188.2, 186.1, 168.4, 166.7, 160.7, 160.2, 154.1 (ddd, *J* = 2.93, 9.54, 247.22 Hz), 152.7, 146.6 (ddd, *J* = 3.67, 12.47, 245.75 Hz), 145.4, 127.9, 127.9, 127.3 - 127.6 (m), 123.5, 123.5, 123.2, 121.9, 121.8, 119.6, 119.4, 117.6 (ddd, *J* = 1.47, 5.14, 20.54

Hz), 116.8 (ddd, *J* = 1.47, 5.14, 20.54 Hz), 106.9, 106.9, 105.0 (dd, *J* = 20.54, 28.61 Hz), 105.0 (dd, *J* = 20.54, 28.61 Hz), 101.6, 101.5, 59.9, 59.6, 49.2, 49.0, 14.0, 13.6; ($\upsilon_{max}$/cm$^{-1}$) 1690, 1630, 1576, 1519, 1509, 1428, 1385, 1365, 1331, 1305, 1255, 1228, 1170, 1135, 1095, 1071, 1028, 967, 879, 812, 783, 741, 658, 627, 584, 567, 510. **See notes A, B**.

Compound **2g**, white solid, 348 mg (81.3% yield); $^{1}$H NMR (400 MHz, $CDCl_3$) δ 11.19 (br. s., 0.9H), 9.70 (br. s., 0.1H), 8.29 (d, *J* = 13.85 Hz, 0.9H), 8.23 (d, *J* = 14.35 Hz, 0.1H), 7.82 - 7.88 (m, 1H), 7.48 - 7.53 (m, 1H), 7.39 - 7.45 (m, 2H), 7.31 (d, *J* = 6.80 Hz, 1H), 7.21 (ddd, *J* = 10.07, 8.81, 6.17 Hz, 1H), 6.87 (ddd, *J* = 10.07, 9.06, 6.29 Hz, 1H), 4.83 - 4.88 (m, 2H), 4.07 (q, *J* = 7.05 Hz, 1.8H), 4.01 (q, *J* = 7.05 Hz, 0.2H), 1.08 (t, *J* = 7.05 Hz, 2.7H), 0.94 (t, *J* = 7.05 Hz, 0.3H); $^{13}$C NMR (101 MHz, $CDCl_3$) δ 188.4, 168.4, 166.6, 160.7, 160.2, 140.5, 138.2, 138.1, 129.6, 126.4, 126.4, 124.9, 124.8, 124.7, 124.6, 124.1, 124.1, 123.4, 123.4, 116.9 (ddd, *J* = 1.47, 5.14, 20.54 Hz), 105.1 (dd, *J* = 21.27, 28.61 Hz), 101.9, 60.0, 59.7, 53.1, 52.9, 14.0, 13.6; ($\upsilon_{max}$/cm$^{-1}$) 1695, 1627, 1573, 1507, 1430, 1383, 1329, 1303, 1256, 1229, 1217, 1171, 1134, 1091, 1070, 1032, 995, 846, 813, 782, 742, 704, 660, 587, 568, 552. **See notes A, B**.

**General Procedure for Compounds 3a – g**. Compound **2a** (1 g, 3.13 mmol, 1 eq.) was dissolved in DCM (7 mL), then DBU (573 µL, 3.83 mmol, 1.2 eq.) and LiCl (270 mg, 6.38 mmol, 2 eq.) were added and the reaction was stirred at 45 °C for 2.5 hours, then at room temperature for 15 hours. Upon completion, the mixture was extracted with DCM (2 x 20 mL) and washed with distilled water (15 mL) with the aqueous phase neutralised using a 1M solution of citric acid (3 mL). The combined organic phases were dried over magnesium sulphate, filtered and concentrated *in vacuo*. The crude product **3a** was used in the successive reaction without further purification. Compound **3a**, pale yellow solid, 1.022 g (>95% crude yield), $^{1}$H NMR (400 MHz, $CDCl_3$) δ 8.55 (s, 1H, H3), 8.20 (dd, *J* = 10.45, 8.69 Hz, 1H, H1), 7.72 (dd, *J* = 11.33, 6.29 Hz, 1H, H2), 4.37 (q, *J* = 7.05 Hz, 2H, H7), 3.41 - 3.48 (m, 1H, H4),

1.32 - 1.43 (m, 5H, H5+6+8), 1.12 - 1.19 (m, 2H, H5+6); $^{13}$C NMR (101 MHz, $CDCl_3$) δ 172.6 (d, *J* = 1.47 Hz), 165.2, 153.3 (dd, *J* = 256.03, 15.41 Hz), 148.8, 148.6 (dd, *J* = 250.89, 13.94 Hz), 137.5 (dd, *J* = 9.54, 2.20 Hz), 125.6 (dd, *J* = 5.13, 2.20 Hz), 115.3 (dd, *J* = 19.07, 2.20 Hz), 110.8, 105.5 (d, *J* = 22.74 Hz), 61.0, 34.8, 14.3, 8.2; ($\upsilon_{max}$/cm$^{-1}$) 1723, 1617, 1602, 1490, 1479, 1454, 1446, 1424, 1396, 1386, 1379, 1335, 1314, 1287, 1228, 1209, 1202, 1167, 1121, 1094, 1054, 1033, 1018, 899, 855, 849, 826, 802, 781, 748, 729, 717, 619, 607, 595, 548, 540; LC-MS retention time 3.28 minutes (method A), purity = 100%, found 294.0 $[M+H]^+$, calculated for $C_{15}H_{13}F_2NO_3$ 294.27 $[M+H]^+$.

Compound **3b**, pale yellow solid, 4.55 g (>95% crude yield), $^1$H NMR (400 MHz, $CDCl_3$) δ 8.47 (s, 1H, H3), 8.27 (dd, *J* = 10.32, 8.81 Hz, 1H, H1), 7.27 (dd, *J* = 11.21, 6.17 Hz, 1H, H2), 4.38 (q, *J* = 7.05 Hz, 2H, H6), 4.21 (q, *J* = 7.22 Hz, 2H, H4), 1.55 (t, *J* = 7.30 Hz, 3H, H5), 1.40 (t, *J* = 7.05 Hz, 3H, H7); $^{13}$C NMR (101 MHz, $CDCl_3$) δ 172.6 (d, *J* = 2.20 Hz), 165.3, 153.5 (dd, *J* = 256.02, 15.41 Hz), 148.7, 148.3 (dd, *J* = 251.62, 13.94 Hz), 135.5 (dd, *J* = 8.80, 2.20 Hz), 126.4 (dd, *J* = 5.13, 2.20 Hz), 115.7 (dd, *J* = 18.34, 2.20 Hz), 111.0, 104.6 (d, *J* = 22.01 Hz), 61.0, 49.3, 14.3, 14.3; ($\upsilon_{max}$/cm$^{-1}$) 1720, 1617, 1566, 1466, 1449, 1375, 1369, 1311, 1288, 1228, 1217, 1209, 1173, 1157, 1137, 1094, 1071, 1049, 1016, 902, 863, 829, 814, 802; LC-MS retention time 3.18 minutes (method A), purity = 100%, found 281.9 $[M+H]^+$, calculated for $C_{14}H_{13}F_2NO_3$ 282.26 $[M+H]^+$.

Compound **3c**, pale yellow solid, 540 mg (57.2% crude yield); $^1$H NMR (400 MHz, $CDCl_3$) δ 8.59 (s, 1H), 8.28 (dd, *J* = 10.45, 8.69 Hz, 1H), 7.38 - 7.41 (m, 2H), 7.33 - 7.43 (m, 3H), 7.09 - 7.20 (m, 3H), 5.35 (s, 2H), 4.40 (q, *J* = 7.22 Hz, 2H), 1.41 (t, *J* = 7.18 Hz, 3H); $^{13}$C NMR (101 MHz, $CDCl_3$) δ 172.7 (d, *J* = 1.47 Hz), 165.2, 153.3 (dd, *J* = 15.41, 256.03 Hz), 149.9, 148.5 (dd, *J* = 13.94, 251.62 Hz), 136.1 (d, *J* = 11.00 Hz), 133.3, 129.6, 128.9, 126.4 (dd, *J* = 2.20, 5.14 Hz), 126.0, 115.6 (dd, *J* = 2.20, 18.34 Hz), 111.1, 105.7 (d, *J* = 22.74 Hz), 61.1, 57.9, 14.3; ($\upsilon_{max}$/cm$^{-1}$) 1718, 1617, 1598, 1492, 1454, 1387, 1287, 1228, 1206, 1168,

1077, 922, 894, 825, 800, 731, 703, 620, 536; LC-MS retention time 3.62 minutes (method A), purity = 100%, found 344.1 $[M+H]^+$, calculated for $C_{19}H_{15}F_2NO_3$ 344.33 $[M+H]^+$.

Compound **3d**, pale yellow solid, 846 mg (89.1% crude yield); $^1$H NMR (400 MHz, $CDCl_3$) δ 8.56 (s, 1H), 8.33 (dd, *J* = 10.32, 8.56 Hz, 1H), 7.88 (dd, *J* = 7.81, 1.01 Hz, 1H), 7.66 (d, *J* = 2.01 Hz, 1H), 7.49 (t, *J* = 7.68 Hz, 1H), 7.41 (dd, *J* = 7.68, 1.13 Hz, 1H), 6.98 (d, *J* = 2.27 Hz, 1H), 6.68 (dd, *J* = 11.08, 6.29 Hz, 1H), 4.39 (q, *J* = 7.05 Hz, 2H), 1.39 (t, *J* = 7.05 Hz, 3H); $^{13}$C NMR (101 MHz, $CDCl_3$) δ 172.9 (d, *J* = 2.20 Hz), 165.0, 153.4 (dd, *J* = 14.67, 256.02 Hz), 149.4, 149.0, 148.7 (dd, *J* = 13.94, 251.62 Hz), 146.6, 137.2 (dd, *J* = 2.20, 9.54 Hz), 130.4, 125.4 - 125.5 (m), 124.6, 124.2, 123.9, 122.9, 115.2 (dd, *J* = 2.20, 18.34 Hz), 111.8, 107.5, 106.3 (d, *J* = 22.74 Hz), 61.2, 14.4; ($\upsilon_{max}$/cm$^{-1}$) 1685, 1646, 1612, 1566, 1491, 1436, 1279, 1211, 1168, 1116, 1085, 1048, 1009, 904, 855, 800, 738, 631, 604, 561; LC-MS retention time 3.78 minutes (method A), purity = 100%, found 370.0 $[M+H]^+$, calculated for $C_{20}H_{13}F_2NO_4$ 370.32 $[M+H]^+$.

Compound **3e**, pale yellow solid, 817 mg (85.8% crude yield); $^1$H NMR (400 MHz, $CDCl_3$) δ 8.56 (s, 1H), 8.32 (dd, *J* = 10.32, 8.56 Hz, 1H), 8.09 (dd, *J* = 7.93, 0.88 Hz, 1H), 7.61 - 7.66 (m, 1H), 7.54 (m, 2H), 7.47 (dd, *J* = 7.55, 0.76 Hz, 1H), 6.64 (dd, *J* = 10.83, 6.42 Hz, 1H), 4.38 (q, *J* = 7.05 Hz, 2H), 1.38 (t, *J* = 7.18 Hz, 3H); $^{13}$C NMR (101 MHz, $CDCl_3$) δ 172.9 (d, *J* = 1.47 Hz), 164.8, 153.5 (dd, *J* = 14.67, 256.03 Hz), 148.8 (dd, *J* = 13.94, 251.62 Hz), 148.7, 142.4, 137.4, 136.5 - 136.6 (m), 134.3, 128.1, 126.5, 125.9, 125.5 (dd, *J* = 2.20, 5.14 Hz), 124.9, 123.4, 115.3 (dd, *J* = 2.20, 19.07 Hz), 112.0, 106.2 (d, *J* = 22.74 Hz), 61.2, 14.3; ($\upsilon_{max}$/cm$^{-1}$) 1729, 1619, 1556, 1492, 1397, 1383, 1318, 1285, 1243, 1217, 1202, 1170, 1072, 1029, 901, 851, 803, 727, 699, 618, 605; LC-MS retention time 3.88 minutes (method A), purity = 100%, found 385.9 $[M+H]^+$, calculated for $C_{20}H_{13}F_2NO_3S$ 386.38 $[M+H]^+$.

Compound **3f**, pale yellow solid, 405 mg (94.3% crude yield); $^1$H NMR (400 MHz, $CDCl_3$) δ 8.77 (s, 1H), 8.22 - 8.30 (m, 1H), 7.68 - 7.71 (m, 1H), 7.62 (d, *J* = 7.81 Hz, 1H), 7.38

(dd, *J* = 11.33, 6.04 Hz, 1H), 7.20 - 7.26 (m, 1H), 7.04 (d, *J* = 7.55 Hz, 1H), 6.82 - 6.86 (m, 1H), 5.61 (s, 2H), 4.41 (q, *J* = 7.05 Hz, 2H), 1.42 (t, *J* = 7.05 Hz, 3H); $^{13}$C NMR (101 MHz, $CDCl_3$) δ 172.8, 165.3, 153.3 (dd, *J* = 13.94, 256.02 Hz), 152.0, 150.2, 148.4 (dd, *J* = 13.94, 251.62 Hz), 145.6, 136.1 (dd, *J* = 1.47, 9.54 Hz), 128.3, 126.3 (dd, *J* = 2.20, 5.14 Hz), 123.5, 122.5, 122.3, 117.0, 115.6 (dd, *J* = 2.20, 18.34 Hz), 111.1, 107.1, 105.4 (d, *J* = 23.47 Hz), 61.1, 53.1, 14.4; ($\upsilon_{max}$/cm$^{-1}$) 1674, 1650, 1612, 1493, 1427, 1317, 1290, 1247, 1220, 1126, 1093, 1031, 905, 874, 827, 802, 784, 750, 724, 711, 631, 606, 555, 525; LC-MS retention time 3.73 minutes (method A), purity = 100%, found 383.9 $[M+H]^+$, calculated for $C_{21}H_{15}F_2NO_4$ 384.35 $[M+H]^+$.

Compound **3g**, pale yellow solid, 290 mg (>95% crude yield); $^1$H NMR (400 MHz, $CDCl_3$) δ 8.69 (s, 1H), 8.26 - 8.32 (m, 1H), 7.84 - 7.90 (m, 1H), 7.53 (d, *J* = 5.54 Hz, 1H), 7.47 (m, 1H), 7.34 - 7.40 (m, 1H), 7.08 (dd, *J* = 11.08, 6.29 Hz, 1H), 6.96 - 7.02 (m, 1H), 5.54 (s, 2H), 4.40 (q, *J* = 7.05 Hz, 2H), 1.41 (t, *J* = 7.18 Hz, 3H); $^{13}$C NMR (101 MHz, $CDCl_3$) δ 172.8 (d, *J* = 1.47 Hz), 165.1, 153.4 (dd, *J* = 15.41, 256.76 Hz), 150.2, 148.6 (dd, *J* = 13.94, 252.36 Hz), 140.9, 136.7, 136.1 - 136.3 (m), 127.3, 126.6, 126.2 - 126.4 (m), 125.1, 124.9, 124.5, 121.8, 115.7 (dd, *J* = 2.20, 18.34 Hz), 111.4, 105.3 (d, *J* = 22.74 Hz), 61.3, 57.0, 14.4; ($\upsilon_{max}$/cm$^{-1}$) 1674, 1647, 1613, 1477, 1395, 1316, 1290, 1223, 1172, 1085, 1051, 830, 802, 786, 680, 605, 564; LC-MS retention time 3.85 minutes (method A), purity = 100%, found 400.1 $[M+H]^+$, calculated for $C_{21}H_{15}F_2NO_3S$ 400.41 $[M+H]^+$.

**General Procedure for Compounds 4a, 4b**. Compound **3a** (700 mg, 2.39 mmol, 1 eq.) was refluxed with concentrated HCl (3.5 mL) and concentrated AcOH (13 mL) for 2.5 hours. The mixture was allowed to cool to room temperature and the resulting precipitate was filtered, washed with distilled water (3 mL) and dried. The crude product **4a** was used in the successive reaction without further purification. Compound **4a**, white solid, 573 mg (90.4% yield); $^1$H NMR (400 MHz, $CF_3CO_2D$) δ 9.43 (s, 1H, H3), 8.41 - 8.52 (m, 2H, H1+2), 4.07 -

4.18 (m, 1H, H4), 1.64 - 1.73 (m, 2H, H5+6), 1.41 - 1.49 (m, 2H, H5+6); $^{13}$C NMR (101 MHz, $CF_3CO_2D$) δ 174.8 (d, *J* = 4.01 Hz), 171.7, 160.1 (dd, *J* = 270.27, 15.26 Hz), 154.6 (dd, *J* = 263.79, 14.50 Hz), 152.7, 142.7 (d, *J* = 10.87 Hz), 120.8 (dd, *J* = 8.20, 1.72 Hz), 115.8 (dd, *J* = 20.79, 3.24 Hz), 110.5 (d, *J* = 23.84 Hz), 106.9, 41.5, 10.0; ($\upsilon_{max}$/cm$^{-1}$) 1719, 1614, 1556, 1421, 1332, 1303, 1289, 1231, 1204, 1056, 1033, 1020, 891, 806, 778, 748, 719, 606; LC-MS retention time 3.37 minutes (method A), purity = 100%, found 265.9 $[M+H]^+$, calculated for $C_{13}H_9F_2NO_3$ 266.22 $[M+H]^+$.

Compound **4b**, pale yellow solid, 2.964 g (73.2% yield); $^1$H NMR (400 MHz, $CF_3CO_2D$) δ 9.36 (s, 1H, H3), 8.39 (t, *J* = 8.43 Hz, 1H, H1), 7.99 (dd, *J* = 9.95, 6.17 Hz, 1H, H2), 4.79 (q, *J* = 7.13 Hz, 2H, H4), 1.66 (t, *J* = 7.05 Hz, 3H, H5); $^{13}$C NMR (101 MHz, $CF_3CO_2D$) δ 171.8 (d, *J* = 4.01 Hz), 169.1, 157.7 (dd, *J* = 270.27, 15.26 Hz), 151.9 (dd, *J* = 263.79, 14.50 Hz), 149.4 (d, *J* = 1.15 Hz), 137.9 (d, *J* = 9.15 Hz), 118.8 (dd, *J* = 7.63, 1.33 Hz), 113.4 (dd, *J* = 20.41, 3.43 Hz), 107.1 (d, *J* = 23.27 Hz), 104.7, 53.4, 12.9; ($\upsilon_{max}$/cm$^{-1}$) 1719, 1617, 1484, 1396, 1385, 1361, 1306, 1289, 1231, 1213, 1094, 1042, 948, 900, 874, 808; LC-MS retention time 3.28 minutes (method A), purity = 100%, found 253.8 $[M+H]^+$, calculated for $C_{12}H_9F_2NO_3$ 254.2 $[M+H]^+$.

**General Procedure for Compounds 4c – g**. Crude compound **3c** (450 mg, 1.31 mmol, 1 eq.) was refluxed with LiOH (157 mg, 6.55 mmol, 5 eq.), water (3.28 mL) and dioxane (6 mL) at 100 °C for 2 hours. The mixture was allowed to cool to room temperature. The resulting precipitate was acidified using 1M HCl, filtered, washed with water (3 mL) and dried *in vacuo*. The crude product **4c** was used in the successive reaction without further purification. Compound **4c**, white solid, 170 mg (41.2% yield); $^1$H NMR (400 MHz, $CF_3CO_2D$) δ 9.39 (s, 1H), 8.45 (t, *J* = 8.39 Hz, 1H), 8.05 (dd, *J* = 10.27, 6.24 Hz, 1H), 7.38 - 7.48 (m, 3H), 7.18 - 7.27 (m, 2H), 5.92 (s, 2H); ($\upsilon_{max}$/cm$^{-1}$) 1718, 1615, 1502, 1465, 1387, 1363, 1287, 1223, 1168, 974, 919, 837, 807, 773, 753, 731, 716, 692, 607, 526, 522; LC-MS retention time 3.70 minutes

(method A), purity = 100%, found 316.0 $[M+H]^+$, calculated for $C_{17}H_{11}F_2NO_3$ 316.28 $[M+H]^+$. **See note C**.

Compound **4d**, white solid, 625 mg (84.4% yield); $^1$H NMR (400 MHz, $CF_3CO_2D$) δ 9.48 (s, 1H), 8.56 (t, *J* = 8.25 Hz, 1H), 8.07 (d, *J* = 7.79 Hz, 1H), 7.53 - 7.68 (m, 3H), 7.33 (dd, *J* = 9.90, 6.24 Hz, 1H), 7.04 (d, *J* = 2.02 Hz, 1H); $^{13}$C NMR (101 MHz, $CF_3CO_2D$) δ 175.7 (d, *J* = 3.82 Hz), 171.6, 160.4 (dd, *J* = 15.64, 271.03 Hz), 154.7 (dd, *J* = 14.31, 263.4 Hz), 153.8, 150.2, 149.8, 142.5 (d, *J* = 10.11 Hz), 133.8, 128.7, 126.8, 124.6, 123.8, 120.8 (d, *J* = 8.39 Hz), 115.5 - 115.7 (m), 111.2 (d, *J* = 23.84 Hz), 109.8, 107.7; ($\upsilon_{max}$/cm$^{-1}$) 1718, 1610, 1492, 1456, 1334, 1290, 1263, 1220, 1208, 1017, 897, 851, 806, 793, 736, 720, 598, 562; LC-MS retention time 3.78 minutes (method A), purity = 100%, found 342.0 $[M+H]^+$, calculated for $C_{18}H_9F_2NO_4$ 342.27 $[M+H]^+$.

Compound **4e**, pale yellow solid, 513 mg (73.6% yield); $^1$H NMR (400 MHz, $CF_3CO_2D$) δ 9.51 (s, 1H), 8.58 (t, *J* = 8.21 Hz, 1H), 8.28 (d, *J* = 8.07 Hz, 1H), 7.77 (t, *J* = 7.84 Hz, 1H), 7.58 - 7.67 (m, 3H), 7.31 (dd, *J* = 9.86, 6.28 Hz, 1H); $^{13}$C NMR (101 MHz, $CF_3CO_2D$) δ 175.6 (d, *J* = 4.20 Hz), 171.3, 161.7 (dd, *J* = 15.64, 271.23 Hz), 154.6 (dd, *J* = 14.11, 264.36 Hz), 153.0, 145.6, 141.4 - 141.6 (m), 138.0, 134.8, 130.0, 128.1, 127.2, 124.5, 120.7 - 120.8 (m), 115.5 (dd, *J* = 3.05, 20.60 Hz), 110.9, (d, *J* = 24.03 Hz), 107.7; ($\upsilon_{max}$/cm$^{-1}$) 1612, 1491, 1477, 1460, 1388, 1279, 1218, 1023, 895, 850, 807, 746, 730, 697, 663, 648, 620; LC-MS retention time 3.93 minutes (method A), purity = 100%, found 357.9 $[M+H]^+$, calculated for $C_{18}H_9F_2NO_3S$ 358.33.33 $[M+H]^+$.

Compound **4f**, white solid, 176 mg (50.0% yield); $^1$H NMR (400 MHz, $CF_3CO_2D$) δ 9.69 (s, 1H), 8.42 (t, *J* = 8.34 Hz, 1H), 8.27 (dd, *J* = 10.41, 6.10 Hz, 1H), 7.68 (d, *J* = 7.34 Hz, 1H), 7.55 (d, *J* = 2.11 Hz, 1H), 7.25 - 7.39 (m, 2H), 6.78 (d, *J* = 2.11 Hz, 1H), 6.21 (s, 2H); ($\upsilon_{max}$/cm$^{-1}$) 1615, 1492, 1431, 1387, 1360, 1286, 1217, 1179, 1124, 1050, 1033, 1020, 957,

919, 903, 873, 840, 807, 740, 700, 607, 526; retention time 3.83 minutes (method A), purity = 100%, found 356.0 $[M+H]^+$, calculated for $C_{19}H_{11}F_2NO_4$ 356.30 $[M+H]^+$. **See note C**.

Compound **4g**, white solid, 170 mg (68.0% yield); $^1$H NMR (400 MHz, $CF_3CO_2D$) δ 9.43 (s, 1H), 8.45 (t, *J* = 8.39 Hz, 1H), 8.10 (dd, *J* = 10.27, 6.24 Hz, 1H), 7.93 (d, *J* = 8.07 Hz, 1H), 7.38 - 7.49 (m, 3H), 7.24 (d, *J* = 7.43 Hz, 1H), 6.16 (s, 2H); $^{13}$C NMR (101 MHz, $CF_3CO_2D$) δ 174.9 (d, *J* = 4.20 Hz), 171.6, 160.0 (dd, *J* = 14.88, 270.84 Hz), 154.4 (dd, *J* = 14.88, 264.36 Hz), 152.6, 144.2, 141.1 - 141.3 (m), 140.1, 128.4, 128.2, 127.6, 127.3, 126.8, 126.0, 121.2 - 121.3 (m), 115.9 (dd, *J* = 3.81, 20.22 Hz), 110.1 (d, *J* = 23.27 Hz), 107.0, 62.9; ($\upsilon_{max}$/cm$^{-1}$) 1617, 1340, 1289, 1213, 1049, 821, 788, 743, 687, 605; LC-MS retention time 3.93 minutes (method A), purity = 100%, found 371.9 $[M+H]^+$, calculated for $C_{19}H_{11}F_2NO_3S$ 372.36 $[M+H]^+$.

**General Procedure for Compounds 5a, 5b**. A mixture of **4a** (500 mg, 1.89 mmol, 1 eq.), tert-butyl piperazine-1-carboxylate (1.06 g, 5.67 mmol, 3 eq.) and potassium carbonate (552 mg, 3.78 mmol, 2 eq.) was stirred in DMF (18 mL) at 140 °C for 15 hours. Upon completion, the mixture was extracted with DCM (2 x 15 mL) and washed with distilled water (10 mL) with the aqueous layer neutralised using a 1M citric acid solution (3 mL). Combined organic layers were dried over magnesium sulphate, filtered and concentrated *in vacuo*. The crude solid was recrystallised from DMF (5 mL) to yield Boc-protected ciprofloxacin. This compound (200 mg, 0.46 mmol, 1 eq.) was then dissolved in dry DCM (7 mL), the mixture cooled to 0 °C and TFA (710 μL, 9.27 mmol, 20 eq.) added, then allowed to warm to room temperature over 2 hours. Upon completion, the solution was concentrated *in vacuo* and washed with toluene (4 x 3 mL). The crude was washed with EtOAc (5 mL) and MeOH (5 mL) to give pure compound **5a**, pale orange solid, 150 mg (34.5% yield over two steps); $^1$H NMR (400 MHz, $CF_3CO_2D$) δ 9.29 (s, 1H, H3), 8.24 (d, *J* = 12.34 Hz, 1H, H1), 7.90 (d, *J* = 6.80 Hz, 1H, H2), 4.03 - 4.12 (m, 1H, H4), 3.90 - 3.99 (m, 4H, H8+9), 3.70 - 3.78 (m, 4H, H10+11),

1.60 - 1.68 (m, 2H, H5+6), 1.34 - 1.43 (m, 2H, H5+6); $^{13}$C NMR (101 MHz, $CF_3CO_2D$) δ 173.2, 172.4, 157.6 (d, *J* = 258.64 Hz), 151.5, 150.5 (d, *J* = 10.87 Hz), 143.5, 117.9 (d, *J* = 10.11 Hz), 114.2 (d, *J* = 25.18 Hz), 108.0, 105.7, 48.5 (d, *J* = 5.34 Hz), 46.8, 40.8, 9.9; ($\upsilon_{max}$/cm$^{-1}$) 1685, 1627, 1612, 1490, 1454, 1341, 1272, 1259, 1184, 1138, 1107, 1056, 1034, 941, 894, 886, 829, 807, 793, 785, 749, 723, 708, 665, 637, 609; LC-MS retention time 2.48 minutes (method A), purity = 100%, found 332.0 $[M+H]^+$, calculated for $C_{17}H_{18}FN_3O_3$ 332.35 $[M+H]^+$.

Compound **5b**, pale brown solid, 44 mg (33.3% yield over two steps); $^1$H NMR (400 MHz, $CF_3CO_2D$) δ 9.30 (s, 1H, H3), 8.29 (d, *J* = 12.09 Hz, 1H, H1), 7.48 (d, *J* = 6.55 Hz, 1H, H2), 4.85 (q, *J* = 7.22 Hz, 2H, H4), 3.91 - 3.99 (m, 4H, H7+8), 3.71 - 3.79 (m, 4H, H9+10), 1.74 (t, *J* = 7.30 Hz, 3H, H5); $^{13}$C NMR (101 MHz, $CF_3CO_2D$) δ 170.3, 169.7, 154.9 (d, *J* = 258.64 Hz), 148.2, 147.9 (d, *J* = 10.68 Hz), 138.8, 115.9 (d, *J* = 9.54 Hz), 111.7 (d, *J* = 27.47 Hz), 104.6, 103.3, 52.6, 45.9 (d, *J* = 6.10 Hz), 44.2, 12.7; ($\upsilon_{max}$/cm$^{-1}$) 1696, 1624, 1610, 1508, 1474, 1453, 1421, 1399, 1382, 1366, 1310, 1265, 1202, 1125, 1104, 1088, 1053, 1033, 990, 934, 916, 900, 828, 808, 797, 748, 720; LC-MS retention time 2.38 minutes (method A), purity = 85.5%, found 320.0 $[M+H]^+$, calculated for $C_{16}H_{18}FN_3O_3$ 320.33 $[M+H]^+$.

**General Procedure for Compounds 5c – 5g**. A mixture of compound **4c** (150 mg, 0.48 mmol, 1 eq.), piperazine (248 mg, 2.88 mmol, 6 eq.) and potassium carbonate (133 mg, 0.96 mmol, 2 eq.) was stirred in DMF (2.5 mL) at 140 °C for 2 hours. Upon completion (as monitored by LC-MS), the mixture was extracted with DCM (2 x 15 mL) and washed with water (10 mL) with the aqueous layer neutralised using a 1M solution of citric acid (2 mL). The combined organic layers were dried over magnesium sulfate and concentrated *in vacuo*. The crude compound was recrystallised from DMF (500 µL) and the crude solid washed with EtOAc (5 mL) and MeOH (5 mL) to give pure compound **5c**, white solid, 140 mg (76.5% yield); $^1$H NMR (400 MHz, $CF_3CO_2D$) δ 9.29 (s, 1H), 8.23 (d, *J* = 12.47 Hz, 1H), 7.41 - 7.47 (m, 3H), 7.39 (d, *J* = 6.88 Hz, 1H), 7.18 - 7.28 (m, 2H), 5.91 (s, 2H), 3.69 - 3.86 (m, 4H), 3.52

- 3.69 (m, 4H); $^{13}$C NMR (101 MHz, $CF_3CO_2D$) δ 173.1, 172.2, 157.2 (d, *J* = 258.06 Hz), 151.4, 149.9 (d, *J* = 10.87 Hz), 141.7, 133.0, 132.3, 132.1, 128.9, 118.3 (d, *J* = 9.92 Hz), 114.0 (d, *J* = 26.13 Hz), 108.4, 105.5, 63.4, 48.1 (d, *J* = 5.53 Hz), 46.4; ($\upsilon_{max}$/cm$^{-1}$) 1622, 1578, 1498, 1447, 1390, 1337, 1278, 1262, 1215, 1199, 1179, 1137, 1032, 943, 825, 800, 778, 741, 696, 625, 536, 516; LC-MS retention time 2.68 minutes (method A), purity = 100%, found 382.0 $[M+H]^+$, calculated for $C_{21}H_{20}FN_3O_3$ 382.41 $[M+H]^+$.

Compound **5d**, white solid, 231 mg (32.2% yield); $^1$H NMR (400 MHz, $CF_3CO_2D$) δ 9.35 (s, 1H), 8.41 (d, *J* = 12.29 Hz, 1H), 8.11 (dd, *J* = 7.79, 0.83 Hz, 1H), 7.71 (d, *J* = 2.20 Hz, 1H), 7.66 (t, *J* = 7.84 Hz, 1H), 7.57 - 7.62 (m, 1H), 7.10 (d, *J* = 2.29 Hz, 1H), 6.83 (d, *J* = 6.88 Hz, 1H), 3.55 - 3.77 (m, 8H); $^{13}$C NMR (101 MHz, $CF_3CO_2D$) δ 173.7, 172.0, 157.4 (d, *J* = 258.45 Hz), 152.4, 150.4 (d, *J* = 10.49 Hz), 150.1, 149.4, 143.1, 133.5, 128.2, 126.6, 124.5, 123.6, 117.7 (d, *J* = 10.87 Hz), 113.8 (d, *J* = 25.37 Hz), 109.7, 108.3, 106.2, 47.9 (d, *J* = 4.77 Hz), 46.3; ($\upsilon_{max}$/cm$^{-1}$) 1595, 1493, 1433, 1379, 1330, 1289, 1259, 1202, 1032, 909, 876, 800, 736, 688, 624, 561, 552; LC-MS retention time 2.72 minutes (method A), purity = 100%, found 408.0 $[M+H]^+$, calculated for $C_{22}H_{18}FN_3O_4$ 408.40 $[M+H]^+$.

Compound **5e**, pale yellow solid, 194 mg (36.4% yield); $^1$H NMR (400 MHz, $CF_3CO_2D$) δ 9.27 (s, 1H), 8.32 (d, *J* = 12.38 Hz, 1H), 8.22 (d, *J* = 8.07 Hz, 1H), 7.72 (t, *J* = 7.84 Hz, 1H), 7.52 - 7.60 (m, 3H), 6.71 (d, *J* = 6.88 Hz, 1H), 3.44 - 3.65 (m, 8H); $^{13}$C NMR (101 MHz, $CF_3CO_2D$) δ 174.0, 172.2, 157.7 (d, *J* = 258.83 Hz), 152.1, 150.7 (d, *J* = 10.30 Hz), 145.8, 142.4, 138.1, 135.3, 130.1, 130.0, 128.5, 127.5, 124.8, 117.8 - 118.0 (m), 114.2 (d, *J* = 27.08 Hz), 108.6, 106.6, 48.1 (d, *J* = 4.77 Hz), 46.6; ($\upsilon_{max}$/cm$^{-1}$) 1722, 1664, 1492, 1454, 1395, 1352, 1326, 1285, 1251, 1100, 1042, 885, 802, 700, 661, 616, 563, 540; LC-MS retention time 2.75 minutes (method A), purity = 100%, found 424.2 $[M+H]^+$, calculated for $C_{22}H_{18}FN_3O_3S$ 424.46 $[M+H]^+$.

Compound **5f**, pale pink solid, 167 mg (94.4% yield); $^{1}$H NMR (400 MHz, $CF_3CO_2D$) δ 9.56 (s, 1H), 8.19 (d, *J* = 12.38 Hz, 1H), 7.63 - 7.74 (m, 1H), 7.49 - 7.63 (m, 2H), 7.29 (d, *J* = 4.22 Hz, 2H), 6.82 (br. s., 1H), 6.18 (s, 2H), 3.65 - 3.77 (m, 4H), 3.54 - 3.65 (m, 4H); $^{13}$C NMR (101 MHz, $(CD_3)_2SO$) δ 176.5, 166.3, 152.8 (d, *J* = 250.44 Hz), 152.0, 150.0, 146.6, 145.4 (d, *J* = 10.30 Hz), 137.6, 127.9, 123.7, 123.5, 121.9, 119.0 (d, *J* = 7.06 Hz), 118.7, 111.3 (d, *J* = 23.08 Hz), 107.3, 107.2, 106.0 (d, *J* = 1.91 Hz), 52.7, 50.4 (d, *J* = 4.77 Hz), 45.1; ($\upsilon_{max}$/cm$^{-1}$) 1624, 1583, 1488, 1448, 1341, 1321, 1262, 1215, 1173, 1032, 1013, 940, 807, 793, 747, 628; LC-MS retention time 2.78 minutes (method A), purity = 100%, found 422.0 $[M+H]^+$, calculated for $C_{23}H_{20}FN_3O_4$ 422.43 $[M+H]^+$.

Compound **5g**, pale yellow solid, 41 mg (23.4% yield); $^{1}$H NMR (400 MHz, $CF_3CO_2D$) δ 9.45 (s, 1H), 8.20 (d, *J* = 12.29 Hz, 1H), 7.91 (d, *J* = 7.70 Hz, 1H), 7.44 - 7.52 (m, 2H), 7.41 (t, *J* = 7.79 Hz, 1H), 7.32 (d, *J* = 6.60 Hz, 1H), 7.19 (d, *J* = 7.34 Hz, 1H), 6.13 (s, 2H), 3.53 - 3.64 (m, 4H), 3.44 - 3.53 (m, 4H); ($\upsilon_{max}$/cm$^{-1}$) 1621, 1583, 1488, 1448, 1338, 1279, 1266, 1204, 1182, 1049, 1032, 940, 825, 793, 744, 689, 622, 554, 517; LC-MS retention time 5.53 minutes (method B), purity = 100%, found 437.9 $[M+H]^+$, calculated for $C_{23}H_{20}FN_3O_3S$ 438.49 $[M+H]^+$. **See note C**.

**General Procedure for Compounds 6a – 6g**. Compound **5a** (150 mg, 0.45 mmol, 1 eq.) was stirred in DCM (7 mL) for 5 minutes (method A), then 4M HCl in dioxane (2.26 mL, 9.05 mmol, 20 eq.) was added dropwise and the mixture stirred for 1 hour. Upon completion, the mixture was washed with hexane (3 x 1 mL) and lyophilised overnight to give compound **6a**, pale brown solid; $^{1}$H NMR (400 MHz, $(CD_3)_2SO$) δ 15.13 (br. s., 1H, H7), 9.46 (br. s., 2H, H13), 8.67 (s, 1H, H3), 7.94 (d, *J* = 13.09 Hz, 1H, H1), 7.61 (d, *J* = 7.30 Hz, 1H, H2), 3.86 (br. s., 1H, H4), 3.53 - 3.60 (m, 4H, H8+9), 3.27 - 3.36 (m, 4H, H10+11), 1.28 - 1.37 (m, 2H, H5+6), 1.15 - 1.24 (m, 3H, H5+6+12); $^{13}$C NMR (101 MHz, $(CD_3)_2SO$) δ 176.4 (d, *J* = 2.93 Hz), 165.9, 152.9 (d, *J* = 249.42 Hz), 148.2, 144.1 (d, *J* = 10.27 Hz), 139.1, 119.3 (d, *J* = 8.07

Hz), 111.2 (d, *J* = 23.47 Hz), 106.9 (d, *J* = 2.93 Hz), 106.8, 46.3 (d, *J* = 5.14 Hz), 42.5, 36.0, 7.6; ($\upsilon_{max}$/cm$^{-1}$) 1701, 1624, 1491, 1458, 1383, 1341, 1272, 1142, 1106, 1034, 941, 909, 889, 853, 829, 804, 774, 749, 703, 665, 636, 619; LC-MS retention time 1.89 minutes (method A) and 4.70 minutes (method B), purity = 97.6% (found 332.1 $[M+H]^+$) and 100% (found 332.0 $[M+H]^+$), respectively, calculated for $C_{17}H_{18}FN_3O_3$ 332.35 $[M+H]^+$; HRMS observed 332.1404 $[M+H]^+$, theoretical value 332.1405 $[M+H]^+$.

Compound **6b**, pale orange solid; $^1$H NMR (400 MHz, $(CD_3)_2SO$) δ 15.31 (br. s., 1H, H6), 9.37 (br. s., 2H, H12), 8.97 (s, 1H, H3), 7.96 (d, *J* = 13.09 Hz, 1H, H1), 7.26 (d, *J* = 7.30 Hz, 1H, H2), 4.62 (q, *J* = 7.13 Hz, 2H, H4), 3.52 - 3.59 (m, 4H, H7+8), 3.25 - 3.33 (m, 4H, H9+10), 1.41 (t, *J* = 7.18 Hz, 3H, H5), 1.22 (d, *J* = 6.55 Hz, 1H, H11); $^{13}$C NMR (101 MHz, $(CD_3)_2SO$) δ 176.3 (d, *J* = 3.05 Hz), 166.3, 152.9 (d, *J* = 249.48 Hz), 148.9, 144.6 (d, *J* = 10.68 Hz), 137.3, 120.1 (d, *J* = 7.63 Hz), 111.6 (d, *J* = 23.65 Hz), 107.3, 106.7 (d, *J* = 3.43 Hz), 49.3, 46.6 (d, *J* = 4.58 Hz), 42.8, 14.6; ($\upsilon_{max}$/cm$^{-1}$) 1701, 1696, 1626, 1507, 1454, 1345, 1340, 1332, 1273, 1130, 1053, 1033, 933, 899, 859, 829, 804, 746, 665; LC-MS retention time 1.89 minutes (method A) and 3.29 minutes (method B), purity = 100% (found 320.1 $[M+H]^+$) and 98.5% (found 320.1 $[M+H]^+$), respectively, calculated for $C_{16}H_{18}FN_3O_3$ 320.34 $[M+H]^+$; HRMS observed 320.1404 $[M+H]^+$, theoretical value 320.1405 $[M+H]^+$.

Compound **6c**, white solid; $^1$H NMR (400 MHz, $(CD_3)_2SO$) δ 15.14 (br. s., 1H), 9.57 (br. s., 1H), 9.19 (s, 1H), 7.92 (d, J = 12.93 Hz, 1H), 7.06 - 7.48 (m, 6H), 5.90 (s, 2H), 3.41 (br. s., 4H), 3.22 (br. s., 4H); $^{13}$C NMR (101 MHz, $(CD_3)_2SO$) δ 176.4 (d, *J* = 1.53 Hz), 166.0, 152.6 (d, *J* = 250.05 Hz), 149.6, 143.9 (d, *J* = 10.11 Hz), 137.5, 135.3, 129.0, 128.2, 127.0, 120.1 (d, *J* = 7.44 Hz), 111.4 (d, *J* = 22.89 Hz), 107.3, 107.2 (d, *J* = 2.86 Hz), 56.5, 46.2 (d, *J* = 4.20 Hz), 42.3; ($\upsilon_{max}$/cm$^{-1}$) 1718, 1627, 1507, 1453, 1383, 1367, 1268, 1254, 1207, 1059, 1033, 1007, 960, 927, 903, 833, 802, 763, 739, 698, 535, 524; LC-MS retention time 2.17 minutes (method A) and 4.24 minutes (method B), purity = 98.9% (found 382.1 $[M+H]^+$) and

98.8% (found 382.1 $[M+H]^+$), respectively, calculated for $C_{21}H_{20}FN_3O_3$ 382.41 $[M+H]^+$; HRMS observed 382.1559 $[M+H]^+$, theoretical value 382.1561 $[M+H]^+$.

Compound **6d**, pale yellow solid; $^1$H NMR (400 MHz, $(CD_3)_2SO$) δ 14.91 (br. s., 1H), 9.31 (br. s., 2H), 8.87 (s, 1H), 8.05 - 8.10 (m, 2H), 8.01 (dd, *J* = 7.81, 1.01 Hz, 1H), 7.74 (dd, *J* = 7.81, 1.01 Hz, 1H), 7.56 (t, *J* = 7.81 Hz, 1H), 7.22 (d, *J* = 2.27 Hz, 1H), 6.37 (d, *J* = 7.30 Hz, 1H), 3.09 - 3.24 (m, 8H); $^{13}$C NMR (101 MHz, $(CD_3)_2SO$) δ 176.8 (d, *J* = 2.20 Hz), 165.4, 153.0 (d, *J* = 250.89 Hz), 149.4, 148.3, 147.5, 144.6 (d, *J* = 11.00 Hz), 138.4, 129.9, 124.2, 123.5, 123.3, 119.4 (d, *J* = 8.07 Hz), 111.5 (d, *J* = 23.48 Hz), 108.2, 107.7, 106.5 (d, *J* = 2.93 Hz), 45.9 (d, *J* = 4.40 Hz), 42.3; ($\upsilon_{max}$/cm$^{-1}$) 1724, 1627, 1505, 1451, 1380, 1331, 1271, 1201, 1172, 1116, 1033, 1017, 908, 871, 804, 734, 625, 559, 549; LC-MS retention time 2.23 minutes (method A) and 5.17 minutes (method B), purity = 100% (both), found 408.1 $[M+H]^+$ (both), calculated for $C_{22}H_{18}FN_3O_4$ 408.40 $[M+H]^+$; HRMS observed 408.1352 $[M+H]^+$, theoretical value 408.1354 $[M+H]^+$.

Compound **6e**, pale orange solid; $^1$H NMR (400 MHz, $(CD_3)_2SO$) δ 9.47 (br. s., 2H), 8.83 (s, 1H), 8.23 (d, *J* = 7.89 Hz, 1H), 8.07 (d, *J* = 12.93 Hz, 1H), 7.89 (d, *J* = 5.41 Hz, 1H), 7.79 - 7.84 (m, 1H), 7.68 - 7.76 (m, 2H), 6.32 (d, *J* = 7.15 Hz, 1H), 3.04 - 3.26 (m, 8H); $^{13}$C NMR (101 MHz, $(CD_3)_2SO$) δ 176.8 (d, *J* = 2.48 Hz), 165.3, 153.0 (d, *J* = 250.05 Hz), 148.5, 144.7 (d, *J* = 10.68 Hz), 142.1, 137.8, 136.3, 133.7, 128.8, 126.1, 126.1, 125.2, 123.9, 119.5 (d, *J* = 7.63 Hz), 111.7 (d, *J* = 23.08 Hz), 108.4, 106.2 (d, *J* = 2.67 Hz), 45.9 (d, *J* = 4.77 Hz), 42.2; ($\upsilon_{max}$/cm$^{-1}$) 1722, 1666, 1627, 1499, 1439, 1396, 1354, 1268, 1181, 1032, 951, 901, 866, 832, 799, 713, 684, 615, 555, 537; LC-MS retention time 2.33 minutes (method A) and 5.27 minutes (method B), purity = 100% (both), found 424.1 $[M+H]^+$ (both), calculated for $C_{22}H_{18}FN_3O_3S$ 424.46 $[M+H]^+$; HRMS observed 424.1124 $[M+H]^+$, theoretical value 424.1126 $[M+H]^+$.

Compound **6f**, pale orange solid; $^{1}$H NMR (400 MHz, $(CD_3)_2SO$) δ 15.11 (br. s., 1H), 9.62 (br. s., 2H), 9.33 (s, 1H), 8.10 (d, *J* = 2.11 Hz, 1H), 7.90 (d, *J* = 13.11 Hz, 1H), 7.65 (d, *J* = 7.52 Hz, 1H), 7.38 (d, *J* = 7.24 Hz, 1H), 7.34 (d, *J* = 7.24 Hz, 1H), 7.28 (t, *J* = 7.57 Hz, 1H), 7.00 (d, *J* = 2.20 Hz, 1H), 6.17 (s, 2H), 3.32 - 3.43 (m, 4H), 3.22 (br. s., 4H); $^{13}$C NMR (101 MHz, $(CD_3)_2SO$) δ 176.4 (d, *J* = 2.48 Hz), 165.9, 152.6 (d, *J* = 249.67 Hz), 152.0, 150.0, 146.5, 143.9 (d, *J* = 10.30 Hz), 137.4, 127.8, 123.9, 123.4, 121.9, 119.9 (d, *J* = 7.63 Hz), 118.5, 111.4 (d, *J* = 22.89 Hz), 107.2, 107.1, 106.8 (d, *J* = 3.05 Hz), 52.5, 46.2 (d, *J* = 4.77 Hz), 42.2; ($\upsilon_{max}$/cm$^{-1}$) 1712, 1624, 1546, 1496, 1448, 1387, 1268, 1209, 1179, 1032, 1015, 932, 801, 756, 741, 557, 525, 510; LC-MS retention time 2.33 minutes (method A) and 4.70 minutes (method B), purity = 100% (both), found 422.1 $[M+H]^+$ (both), calculated for $C_{23}H_{20}FN_3O_4$ 422.43 $[M+H]^+$; HRMS observed 422.1507 $[M+H]^+$, theoretical value 422.1511 $[M+H]^+$.

Compound **6g**, red solid; $^{1}$H NMR (400 MHz, $(CD_3)_2SO$) δ 15.11 (br. s., 1H), 9.31 (s, 1H), 9.24 (br. s., 2H), 7.95 (d, *J* = 13.11 Hz, 1H), 7.91 (d, *J* = 7.15 Hz, 1H), 7.78 (d, *J* = 5.41 Hz, 1H), 7.53 (d, *J* = 5.50 Hz, 1H), 7.36 - 7.47 (m, 2H), 7.15 (d, *J* = 7.34 Hz, 1H), 6.16 (s, 2H), 3.24 - 3.30 (m, 4H), 3.16 (br. s., 4H); $^{13}$C NMR (101 MHz, $(CD_3)_2SO$) δ 176.6 (d, *J* = 2.48 Hz), 166.0, 152.7 (d, *J* = 250.05 Hz), 150.4, 143.8 (d, *J* = 10.30 Hz), 140.8, 137.8, 136.8, 129.2, 127.7, 125.1, 124.6, 124.2, 123.7, 119.9 (d, *J* = 7.82 Hz), 111.6 (d, *J* = 23.08 Hz), 107.4, 106.9 (d, *J* = 1.53 Hz), 56.7, 46.2 (d, *J* = 49.6 Hz), 42.4; ($\upsilon_{max}$/cm$^{-1}$) 1707, 1617, 1507, 1395, 1300, 1268, 1206, 1107, 1056, 1033, 940, 832, 802, 771, 725, 699, 620, 554, 516; LC-MS retention time 2.40 minutes (method A) and 4.81 minutes (method B), purity = 100% (both), found 438.1 $[M+H]^+$ (both), calculated for $C_{23}H_{20}FN_3O_3S$ 438.49 $[M+H]^+$; HRMS observed 438.1278 $[M+H]^+$, theoretical value 438.1282 $[M+H]^+$.

**Notes**

A) Compounds **2a-g** display complex and unusual splitting patterns and integrals in their associated NMR spectra. Since fluorine-decoupled carbon-13 NMR spectra could not be generated, the highly fluorinated nature of the aromatic rings in these compounds causes splitting of the signals of nearby carbons. Additionally, compounds **2a-g** can all form two distinct structural isomers due to their common 3-aminoacrylate moiety. These pairs of isomers exist in equilibrium with an interconversion rate significantly less than the difference in frequency between the isomers ('slow on the NMR timescale') meaning that both isomers are fully resolved in $^{1}H$ and $^{13}C$ NMR spectra.

B) *Continuing from note A*; the reduction in signal-to-noise ratio caused by the high degree of splitting of aromatic carbon signals, in combination with the twinning of each peak, precluded resolution of many of these peaks for some compounds. In some cases, several small baseline multiplets are visible in the correct chemical shift range and are most likely the aforementioned missing signals.

C) Poor compound solubility in all deuterated solvents tested precluded analysis *via* carbon-13 NMR.

## AUTHOR INFORMATION

### Corresponding Author

*Please direct all correspondence to k.miraz.rahman@kcl.ac.uk and mark.sutton@phe.gov.uk.

### Author Contributions

M.L. wrote the manuscript with input from all authors; M.L. and A.F. undertook the synthesis, purification and characterisation of compounds; C.H., B.E. and M.C. carried out the microbiological evaluation of the compounds; S.J. completed the computational modelling work; K.M.R. and J.M.S. conceived of, supervised and oversaw completion of the project.

### Competing Interests

The authors declare no competing financial interest.

## ACKNOWLEDGEMENTS

The authors would like to thank the BBSRC (grant reference BB/M015033/1) and Public Health England Pipeline (project code 109994) for funding this research.

### Supplementary Materials

The following materials are available online: characterisation data for new N1-benzofused fluoroquinolones, tabular data for modelled N1-benzofused fluoroquinolone-DNA gyrase interactions and top binding poses for compounds **6a**, **6e** and **6g** docked against *S. aureus* DNA gyrase.

## ABBREVIATIONS

ATCC, American Type Culture Collection; DNA, deoxyribonucleic acid; HRMS, high resolution mass spectrometry; IR, infrared spectroscopy; LC-MS, liquid chromatography-mass spectrometry; MIC, minimum inhibitory concentration; NCTC, National Collection of Type Cultures; NMR, nuclear magnetic resonance; PAβN, phenylalanine-arginine beta-naphthylamide; PMBN, polymyxin B nonapeptide; TLC, thin layer chromatography.

## REFERENCES


1. Dauter, Z.; Wlodawer, A., Progress in protein crystallography. *Protein Pept Lett* **2016,** *23* (3), 201-10.
2. Sliwoski, G.; Kothiwale, S.; Meiler, J.; Lowe, E. W., Jr., Computational methods in drug discovery. *Pharmacol Rev* **2014,** *66* (1), 334-95.
3. Chaskar, P.; Zoete, V.; Rohrig, U. F., On-the-Fly QM/MM Docking with Attracting Cavities. *J Chem Inf Model* **2017,** *57* (1), 73-84.
4. *Fluoroquinolone Antibiotics*. 1st ed.; Springer Basel AG: Basel, 2003.
5. *Antibacterial Drugs - Global Industry Analysis, Size, Share, Growth, Trends and Forecast, 2015-2023*; Transparency Market Research: 2016.
6. Lesher, G. Y.; Froelich, E. J.; Gruett, M. D.; Bailey, J. H.; Brundage, R. P., 1,8-Naphthyridine Derivatives. A New Class of Chemotherapeutic Agents. *J Med Pharm Chem* **1962,** *91*, 1063-5.
7. Andersson, M. I.; MacGowan, A. P., Development of the quinolones. *J Antimicrob Chemother* **2003,** *51 Suppl 1*, 1-11.
8. *Progress in Medicinal Chemistry*. 1st ed.; Elsevier Publications: Waltham, 2015.
9. Tanne, J. H., FDA adds "black box" warning label to fluoroquinolone antibiotics. *BMJ* **2008,** *337*, a816.
10. Mandell, L.; Tillotson, G., Safety of fluoroquinolones: An update. *Can J Infect Dis* **2002,** *13* (1), 54-61.
11. Chan, T.; Bunce, P. E., Fluoroquinolone antimicrobial drugs. *CMAJ* **2017,** *189* (17), E638.
12. Bassetti, M.; Righi, E.; Pecori, D.; Tillotson, G., Delafloxacin: an improved fluoroquinolone developed through advanced molecular engineering. *Future Microbiol* **2018,** *13*, 1081-1094.
13. Cable, H. Antibiotics Currently in Global Clinical Development (accessed 27/05/2019).
14. Drlica, K.; Hiasa, H.; Kerns, R.; Malik, M.; Mustaev, A.; Zhao, X., Quinolones: action and resistance updated. *Curr Top Med Chem* **2009,** *9* (11), 981-98.
15. Drlica, K.; Malik, M.; Kerns, R. J.; Zhao, X., Quinolone-mediated bacterial death. *Antimicrob Agents Chemother* **2008,** *52* (2), 385-92.
16. Hooper, D. C., Mode of action of fluoroquinolones. *Drugs* **1999,** *58 Suppl 2*, 6-10.
17. Hooper, D. C., Mechanisms of action of antimicrobials: focus on fluoroquinolones. *Clin Infect Dis* **2001,** *32 Suppl 1*, S9-S15.
18. Anderson, V. E.; Osheroff, N., Type II topoisomerases as targets for quinolone antibacterials: turning Dr. Jekyll into Mr. Hyde. *Curr Pharm Des* **2001,** *7* (5), 337-53.
19. Llorente, B.; Leclerc, F.; Cedergren, R., Using SAR and QSAR analysis to model the activity and structure of the quinolone-DNA complex. *Bioorg Med Chem* **1996,** *4* (1), 61-71.

20. Domagala, J. M., Structure-activity and structure-side-effect relationships for the quinolone antibacterials. *J Antimicrob Chemother* **1994,** *33* (4), 685-706.
21. Tetko, I. V.; Gasteiger, J.; Todeschini, R.; Mauri, A.; Livingstone, D.; Ertl, P.; Palyulin, V. A.; Radchenko, E. V.; Zefirov, N. S.; Makarenko, A. S.; Tanchuk, V. Y.; Prokopenko, V. V., Virtual computational chemistry laboratory--design and description. *J Comput Aided Mol Des* **2005,** *19* (6), 453-63.
22. Maxwell, A.; Burton, N. P.; O'Hagan, N., High-throughput assays for DNA gyrase and other topoisomerases. *Nucleic Acids Res* **2006,** *34* (15), e104.
23. Masci, D.; Hind, C.; Islam, M. K.; Toscani, A.; Clifford, M.; Coluccia, A.; Conforti, I.; Touitou, M.; Memdouh, S.; Wei, X.; La Regina, G.; Silvestri, R.; Sutton, J. M.; Castagnolo, D., Switching on the activity of 1,5-diaryl-pyrrole derivatives against drug-resistant ESKAPE bacteria: Structure-activity relationships and mode of action studies. *Eur J Med Chem* **2019,** *178*, 500-514.

**For Table of Contents Only**

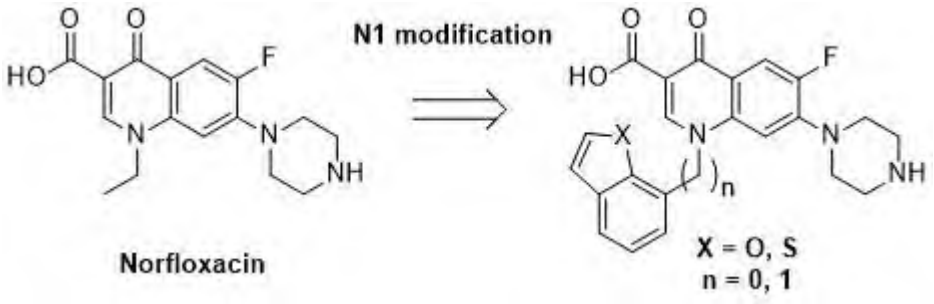


Norfloxacin